Rowan University

Rowan Digital Works

Theses and Dissertations

5-14-2021

Effects of genipin crosslinking on the properties of tendon derived extracellular matrix hydrogels

Alicia Cheyenne Coombs
Rowan University

Follow this and additional works at: https://rdw.rowan.edu/etd

 Part of the Biomedical Engineering and Bioengineering Commons

Recommended Citation

Coombs, Alicia Cheyenne, "Effects of genipin crosslinking on the properties of tendon derived extracellular matrix hydrogels" (2021). *Theses and Dissertations*. 2901.
https://rdw.rowan.edu/etd/2901

This Thesis is brought to you for free and open access by Rowan Digital Works. It has been accepted for inclusion in Theses and Dissertations by an authorized administrator of Rowan Digital Works. For more information, please contact graduateresearch@rowan.edu.

www.manaraa.com

EFFECTS OF GENIPIN CROSSLINKING ON THE PROPERTIES OF TENDON DERIVED EXTRACELLULAR MATRIX HYDROGELS

by

Alicia Cheyenne Coombs

A Thesis

Submitted to the
Department of Biomedical Engineering
College of Engineering
In partial fulfillment of the requirement
For the degree of
Master of Science in Biomedical Engineering
at
Rowan University
May 7, 2021

Thesis Chair: Vince Beachley, Ph.D.

Committee Members:
Peter Galie, Ph.D.
Sebastian Vega, Ph.D.

www.manaraa.com

© 2021 Alicia Cheyenne Coombs

www.manaraa.com

Dedications

I would like to dedicate this manuscript to my closest family and friends.

www.manaraa.com

Acknowledgments

I would first like to thank my advisor and thesis chair, Dr. Vince Beachley, for his continuous guidance and support throughout my undergraduate and graduate research. He has provided me with the wisdom and knowledge to be successful in my research and future endeavors. I would also like to express my appreciation to my committee members, Dr. Peter Galie and Dr. Sebastian Vega for all their guidance, knowledge and support throughout the duration of my undergraduate and graduate careers.

In addition, I would like to thank my closest friends that I have met during my time at Rowan, Rebecca Charboneau and Brandon Deore. My friends have provided me with constant support throughout the years which I value greatly.

Finally, I would like to acknowledge my family who have supported me in everything I have attempted and have given me unconditional guidance and love. Through their constant support, I have learned the true meaning of the phrase "You can do anything if you set your mind to it.".

www.manaraa.com

Abstract

Alicia Cheyenne Coombs
EFFECTS OF GENIPIN CROSSLINKING ON THE PROPERTIES OF TENDON DERIVED EXTRACELLULAR MATRIX HYDROGELS
2020-2021
Vince Beachley, Ph.D.
Master of Science in Biomedical Engineering

Extracellular matrix (ECM) hydrogels are a useful biomaterial in the tissue engineering field used for injectables in drug delivery systems, wound dressing, tissue regeneration and many other applications. ECM hydrogels are highly biocompatible, contain proper ratios of biomolecules required for complex bioactivity of tissues and they promote tissue repair. However, ECM hydrogels typically have poor mechanical strength, which leads to hydrogel instability, and a limitation in their ability to be modified for translational applications. In this research, genipin, a natural crosslinker derived from plants, was utilized in an attempt to improve upon the mechanical limitations of ECM hydrogels. Genipin has a low toxicity that is reportedly 10,000x less than that of glutaraldehyde, another chemical that is commonly used in biofabrication for crosslinking purposes. In this research, improved mechanical properties and enhanced resistance to degradation were observed with increasing ECM and genipin concentrations. 2D and 3D genipin crosslinked dECM hydrogels seeded with mesenchymal stem cells displayed viability at all time points. Cells were viable in hydrogels containing genipin up to 1mM, however over time there was a noticeable decrease in cell count above 0.1mM genipin concentrations. These results indicates that genipin crosslinking may provide a wide range of benefits for ECM hydrogels and may be a viable alternative for more toxic crosslinkers such as glutaraldehyde.

www.manaraa.com

Table of Contents

www.manaraa.com

Table of Contents (Continued)

www.manaraa.com

Table of Contents (Continued)

www.manaraa.com

List of Figures

www.manaraa.com

List of Figures (Continued)

Figure Page

www.manaraa.com

Chapter 1

Literature Review

1.1 Introduction

The most long-standing goal in regard to tissue engineering and regenerative medicine has been to adequately and efficiently develop mechanisms and platforms that can be used to improve the lives of those who are suffering from debilitating medical conditions and diseases. In the fields of tissue engineering and regenerative medicine, one of the most well studied biological platforms utilized to tackle this issue are hydrogels.

Hydrogels are three-dimensional (3D) matrices consisting of highly hydrophilic natural or synthetic materials. One of the most notable features of hydrogels is their ability to absorb large amounts of fluids within the 3D network. This unique property is often attributed to the extensive hydrophilic properties of hydrogels [1]. The first mention of hydrogels for biomedical applications was in a ground-breaking paper published by Wichterle and Lim where they identified a polymer-based hydrogel (poly-2-hydroxyethylmethacrylate (PHEMA)) that had the potential to be used in the biofabrication of contact lenses [2]. The hydrogels described by Wichterle and Lim were the very first biomaterial ever designed specifically for human utilization. Since then, hydrogels have quickly gained traction as an attractive option for other relevant biomedical applications. Hydrogels are now commonly used for the controlled delivery of drugs and therapeutics as well as scaffolds that can promote cell proliferation and enhance tissue regeneration for wound healing applications [3]. Furthermore, hydrogels have also been gaining ground in the development of biosensors. In this application, hydrogels are able to sense and adequately identify biological interactions via bioreceptors [4]. The main

www.manaraa.com

bioreceptors in consideration of hydrogel biosensors include nucleic acids, enzymes and antibodies, each of which has their respective advantages and disadvantages.

Hydrogels are typically classified based on numerous properties such as the origin of the material that makes up the complex 3D matrices whether it be natural or synthetic. Other properties used to classify hydrogels include charge distribution, physical structure, the method of preparation and mechanical strength [5]. In regard to determining if a hydrogel is considered synthetic or natural based, it is contingent on the material source that makes up the 3D network. In the next section, the difference between synthetic and natural hydrogels will be discussed in detail as well as their respective properties and applications.

1.2 Overview of Hydrogels as Biomaterials

1.2.1 Synthetic Hydrogels

Synthetic hydrogels are 3D matrices formulated with hydrophilic homopolymers or copolymers. The 3D networks that make up synthetic hydrogels are formed when the polymers within the network react with each other leading to crosslinks between the molecules by either chemical covalent or physical non-covalent bonds [6]. Some of the most frequently investigated and utilized polymers for fabrication of synthetic hydrogels include, Poly(ethylene glycol) (PEG), Poly (vinyl alcohol) (PVA), and PHEMA [6][7-10].

1.2.2 Naturally Derived Hydrogels

The second classification of hydrogel biomaterials are natural hydrogels. Hydrogels are categorized as natural when the complex network consists of material derived from collagen, gelatin, chitosan, hyaluronic acid or decellularized tissues [5, 11]. Collagen is the most prominent building block that makes up the extracellular matrix of natural tissue and

www.manaraa.com

it plays a key role in providing structural support and remodeling of the ECM [12, 13]. Another main component of the extracellular matrix is hyaluronic acid (HA), a key molecule linked to tissue regeneration and wound healing [14]. For example, HA plays a large role in inflammation, scar formation and angiogenesis, all of which are major steps in the tissue repair process [15]. The properties associated with the previously mentioned hydrogel networks are crucial for tissue regeneration which makes their utilization in hydrogel biofabrication an attractive option.

1.2.3 Hydrogel Materials and Applications

A major requirement in 3D hydrogel fabrication for biomedical applications such as tissue regeneration is that they must allow for the growth and proliferation of cells within the 3D matrix. In order for this to occur, numerous considerations must be considered when formulating hydrogel matrices for specific applications. Firstly, hydrogels for biomedical and translational applications should be biocompatible and induce a minimal immune response [16]. Hydrogels that are biocompatible are crucial for preventing the body from marking the 3D matrix as foreign and inducing harmful inflammatory side effects. In addition, hydrogels should be biodegradable such that removal procedures and invasive surgeries are avoided [17]. Furthermore, the applications for which these complex networks are best suited for revolve around the difference in physical and mechanical properties of synthetic and natural hydrogels.

When it comes to naturally derived hydrogels, they are typically harnessed when the goal of the project involves guiding cells toward a specific lineage as well as tissue regrowth [5]. Often times, naturally derived hydrogels containing extracellular matrix require decellularization which is a critical step to ensure a minimally induced foreign body

www.manaraa.com

response which commonly leads to rejection. Decellularization is a process which kills and removes all cellular components from a donor tissue source while continuously maintain the crucial ratios of natural components within the ECM and the tissues biological activity and function. Decellularization can be achieved through various methods such as mechanical forces, chemical surfactants, enzymatic degradation as well as tissue treatment with acids [18].

On the other hand, synthetic hydrogels are typically used for hydrophilic drug delivery systems and encapsulation of therapeutics. Synthetic hydrogels are favored for such applications due to their versatile and tunable properties that can influence the drug release profiles. In addition to drug delivery, synthetic hydrogels are commonly employed for injectable implants and wound healing applications [19]. Furthermore, synthetic gels are used for developing contact lenses due to their ability to retain moisture and high-water content which provides continuous comfort for long periods of time [20].

1.3 Properties of Hydrogels

1.3.1 Synthetic Hydrogels

There are numerous benefits for utilizing synthetic hydrogels for biomedical applications. Synthetic polymer hydrogels are advantageous because they can be fabricated to exhibit the desired mechanical strength for a given application. In addition, synthetic hydrogels are hydrophilic which allows for enhanced water absorbability and an increased shelf-life compared to hydrogels derived from naturally sourced materials [21]. Although these materials show promise, synthetic polymers fail to properly mimic the natural microenvironment that contains the proper ratios of crucial inert biomolecules. Therefore, synthetic hydrogels must be modified to promote cell adhesion and attachment which may

www.manaraa.com

prevent cellular processes from being able to properly occur. Limited cell adhesion and attachment therefore leads to a reduction and difficulty in restoring damaged tissue and tissue regeneration [6]. In addition, many synthetic polymers used in hydrogel fabrication are not biodegradable which may lead to complications during *in vivo* testing [22, 23].

1.3.2 Naturally Derived Hydrogels

It is important that the materials being utilized to aid in tissue repair closely mimic the natural microenvironment that a cell would experience *in vivo*. Therefore, hydrogels derived from natural materials such as gelatin, chitosan or decellularized tissues may provide an advantage to synthetic hydrogels [16]. In comparison to synthetic hydrogels, hydrogels derived from natural ECM provide cells with a complex structure complete with the necessary biomolecules that are necessary for the complex bioactivity of natural tissue. In addition, ECM hydrogels typically have low toxicity, high biocompatibility, and also have the ability to degrade[11, 24]. However, natural hydrogels derived from ECM also have their limitations. One major limitation of ECM hydrogels is that they lack mechanical strength and durability. The inability of ECM hydrogels to maintain structural integrity limits their potential for biomedical applications. it is important that any hydrogel limitations be identified and properly addressed because the physiochemical properties of a hydrogel will determine their potential for various applications.

www.manaraa.com

1.4 Modification of Hydrogels

1.4.1 Hydrogel Crosslinking

One technique that is commonly utilized to improve upon the lack of mechanical strength observed in hydrogels is crosslinking of the 3D network. The process of crosslinking is the result of inter and intramolecular interactions leading to the polymerization of the formation of bonds, linking one chain of polymer to another [25]. There are multiple strategies that have been employed to crosslink hydrogels which includes various chemical and physical techniques. A detailed review of the various methods and techniques employed in the physical and chemical crosslinking of hydrogels will be discussed within the next two subsections.

1.4.1.1 Physical Crosslinking. A hydrogel is described as being physically crosslinked when the binding between the intramolecular structure within the complex network are reversible[26]. One of the major advantages to using physical crosslinkers is that they avoid the potential risk of cytotoxicity in comparison to chemical crosslinking methods. The most noteworthy bonds that establish physical crosslinks within the 3D network are via crystallization, ionic interactions, hydrogen bonding and interactions of amphiphilic block and graph copolymers [27, 28].

Physical crosslinking via crystallization occurs when an aqueous solution of a given polymer undergoes frequent, ultra-low freezing followed by thawing cycles. The end result of undergoing numerous freeze-thawing cycles produces a highly crosslinked hydrogel with complex crystalline structures located throughout the 3D matrix. In a study investigating the structure and characterization of freeze-dried PVA hydrogels, a direct relationship was observed between increasing PVA concentrations and degree of

www.manaraa.com

crystallinity and the resulting stability of the hydrogel [29]. Additionally, Pianzo, *et. al.* demonstrated the ability to develop chitosan-PVA hydrogels using a freeze-thawing technique which led to modifications to the hydrogel's characteristics. One of which was increased swelling ratio of the hydrogel at a significantly low temperature [30].

Furthermore, physical crosslinking can occur when two oppositely charged molecules within a hydrogel network result in ionic interactions leading to physical bonds developing between the polymer chains. In a study lead by Moura *et. al.* chitosan hydrogels were formed via reversible ionic bonds between glycerol and phosphate molecules and in an additional experimental group, covalently formed via genipin crosslinking [31]. The results indicate that ionic interactions can successfully produce stable hydrogels that display enhanced water retention abilities and improved mechanical properties. In a similar study, chitosan was crosslinked ionically with a glycerol-phosphate solution which demonstrated a unique ability of the hydrogel to maintain a liquid formulation at room temperature followed by a transition to a solid structure when heated to a temperature above 25 °C [32]. One of the major advantages to physical crosslinking of hydrogel networks via ionic interactions is the ability for the gel to be subjected to high amounts of stress, withstand that stress and return to its natural state once the stress has been removed.

Hydrogen bonding is another viable method for crosslinking hydrogels. Although hydrogen bonding by itself may form weaker noncovalent bonds compared to other types of bonds, when a large amount of hydrogen bonds form at once, they can display similar strengths of that found in covalent bonds [33]. Dai *et. al*. established a supramolecular polymer hydrogel reinforced with diaminotriazine-diaminotriazine (DAT-DAT) hydrogen bonds [34]. The hydrogel under investigation displayed enhanced stability as well as

www.manaraa.com

compressive and tensile strength which was attributed to the hydrogen binding throughout the hydrogel network. This was just one of many cases demonstrating the ability of hydrogen bonding to improve hydrogel mechanics. This is worth noting due to the fact that physical crosslinking does not lead to cytotoxic side effects and poor biodegradability which is commonly observed with chemically crosslinked 3D networks.

Furthermore, physically crosslinking of hydrogel matrices can be achieved by incorporation of amphiphilic block and graft copolymers into the network. Amphiphilic block or graft copolymers are known to form structure such as micelles when present in an aqueous solution [35]. Hydrogels formed with block and graft copolymers assemble when the hydrophilic and hydrophobic groups within the polymers form physical bonds and the gel-to-sol temperature (USCT) has been reached. The most common polymers that are utilized to formulate hydrogels using this method include PEG and PLGA due to their biodegradability and biocompatibility [28]. Moffito *et. al*. conducted an in-depth review of thermosensitive block copolymers consisting of PCL and PEG for formulating hydrogels with enhanced properties that are derived from alternating polymer structures [36]. PCL-PEG-PCL copolymer hydrogels demonstrated improved strength and slower rates of degradation compared to PEG-PCL-PEG. In addition, PEGL/PCL copolymer hydrogels formed in a multiblock formation demonstrated an improved level of stability compared to their tri-block counterpart. This finding was attributed to limited crystallization formation within the hydrogel network. The hydrophobic and hydrophilic interactions that occurs within hydrogels formulated with amphiphilic block and graft copolymers leads to improvements in degradation rates and encapsulation. The crucial characteristics are some

www.manaraa.com

of the main reasons why block and graph copolymer hydrogels are an attractive biomaterial in tissue and regenerative engineering, specifically for therapeutic drug delivery [37].

1.4.1.2 Chemical Crosslinking. Chemical crosslinking is the result of irreversible covalent bonds that form within a hydrogel network. Extensive research has been conducted to identify the various ways in which materials such as hydrogels can be chemically crosslinked.

Hydrogel crosslinking via photo-initiated polymerization occurs when unsaturated groups are present within the hydrogel solution. The most common unsaturated group are methacrylates. Methacrylates consist of double bonded carbon groups which, when exposed to visible or UV light will consistently react and form free radicals that can induce polymerization and crosslinking of the hydrogel [38]. Photopolymerization typically requires the use of a photoinitiator, such as eosin-Y, lithium phenyl-2,4,6-trimethyl-benzoylphosphinate (LAP) and riboflavin [39-41]. The photoinitators previously mentioned allow for copious amounts of light to be absorbed at specific wavelengths along the UV and visible light spectrum resulting in the simultaneous formation of free radical groups. These radical groups are what drive the reaction and eventually lead to the polymerization of the hydrogel network. One of the biggest drawbacks of photopolymerization as a technique to chemically crosslink hydrogels is the possibility of DNA becoming damaged from high levels of exposure to UV radiation [42]. Therefore, scientists have increasingly began to identify alternative options and instead utilize photopolymerization techniques which incorporate visible light rather than UV light for initiation of the chemical reaction. A noteworthy attribute of photopolymerization is that the desired site for crosslinking can be specifically selected because when the hydrogel

www.manaraa.com

undergoes exposure to light, only the exposed areas will experience crosslinking [27]. In addition, other characteristics of hydrogel can be altered such as the mechanical properties by controlling the rate of crosslinking reactions.

Chemical crosslinking can also be inspired by enzyme driven reactions. There are countless benefits to an enzymatically driven crosslinking technique, one of which is the rapid gelation time in comparison to other, non-enzyme crosslinked hydrogels [43]. Furthermore, crosslinking with enzymes such as horseradish peroxide (HR) and hydrogen peroxide (H_2O_2) have been proven to be a viable, non-cytotoxic alternative to other crosslinking methods that result in high levels of cytotoxicity [44]. In addition, the hydrogel kinetics can be controlled by direct alteration of the enzyme concentration that is available during the reaction phase of hydrogel fabrication [45].

Chemical crosslinking can also be conducted by reactions between the functional groups of the water-soluble polymers. Some of the most commonly utilized chemical reactions for crosslinking include aldehyde reactions and addition reactions. Crosslinking with aldehydes can be a tedious process and often requires extreme conditions such as high temperature and/or low pH and may include methanol or ethanol. Dai et.al formulated PVA hydrogels that were crosslinked via aldehyde addition [46]. The crosslinking method demonstrated was simple and no harmful biproducts were created in the process. A noticeable increase in rigidity of the PVA hydrogels was observed specifically on the sides exposed to glutaraldehyde (GTA). This finding demonstrates the ability that aldehyde crosslinkers can be utilized to improve the stability of hydrogels as well as their overall stiffness.

www.manaraa.com

Although aldehyde crosslinking is beneficial in term of the hydrogels strength and ability to be fixed for a given period of time, certain aldehydes such as glutaraldehyde have been known to be cytotoxic to cells seeded within the hydrogel network. Gough et. al demonstrated that glutaraldehyde crosslinked collagen/PVA hydrogels could be fabricated however, high toxicity to cells were observed due to the glutaraldehyde crosslinking [47]. The increased toxicity resulted in the high rates of apoptosis and limited biocompatibility.

In addition to aldehyde reactions, crosslinking of hydrogels can be achieved by Michael addition reactions. Michael type addition reactions typically involve nucleophiles (Michael donors) and activated electrophiles (Michael acceptors) [48]. In this reaction, the nucleophile is attached by a carbon-carbon bond. The most common donors involved in Michael addition reactions are enolates, amines and thiol. As for Michael acceptors, molecules that typically contain functional groups such as methacrylates, acrylamides and maleimides are frequently utilized [49, 50]. Michael type additions can be performed with less extreme conditions compared to enzymatic crosslinking which is advantageous for its utilization in biomedical applications. In addition, Michael addition reactions tend to have favorable reaction rates and have also been linked to successful click chemistry reactions [51].

In this research, a chemical crosslinking approach is employed to crosslink bovine derived decellularized ECM hydrogels. Genipin is a chemical compound, with a chemical formula of $C_{11}H_{14}O$ that can be extracted from the fruit, Gardenia Jasminoides (Figure 1).

www.manaraa.com

Figure 1

Molecular structure of the chemical crosslinker Genipin

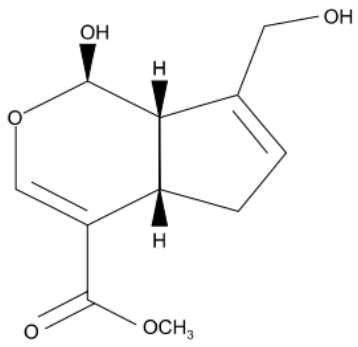

*Note***.** Figure adapted from open access article (CC BY-NC 3.0)[52].

It has previously been reported numerous times as a natural crosslinker for collagen, gelatin, and fibrin derived hydrogels [53-56]. The mechanism behind genipin crosslinking was first described by Touyama et. al. with methylamines as a Michael-type addition reaction[57]. The proposed mechanism for the crosslinking of methylamine with genipin can be visualized (Figure 2) followed by the genipin crosslinking of collagen molecules (Figure 3). Touyama *et. al*. were the first to hypothesize that the spontaneous reaction linked to genipin occurred first by a nucleophilic attack of a primary amine group on the third carbon (C3) of the genipin molecule. The attack on the primary amine lead to a corresponding dihydropyran ring opening followed by a secondary attack on the aldehyde group. The final step to complete the crosslinking mechanism is proposed to be dimerization which leads to the formation of free radical groups [58, 59]. It is hypothesized that the proposed mechanism behind genipin/methylamine crosslinking will be observed

www.manaraa.com

when genipin is reacted with other molecules containing primary amine groups such as collagen and gelatin.

Figure 2

Touyama et. al. proposed mechanism for the crosslinking reactions of genipin and methylamine

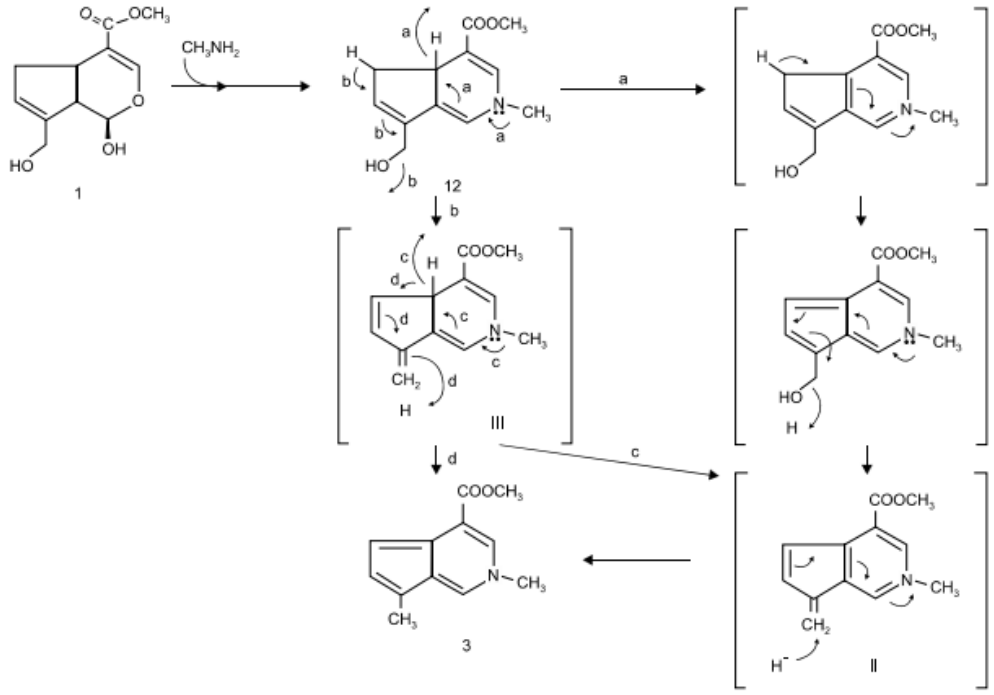

Note. Figure adapted from open access article (CC BY-NC 3.0)[52].

www.manaraa.com

Figure 3

Proposed Mechanism of Genipin crosslinking of two collagen molecules

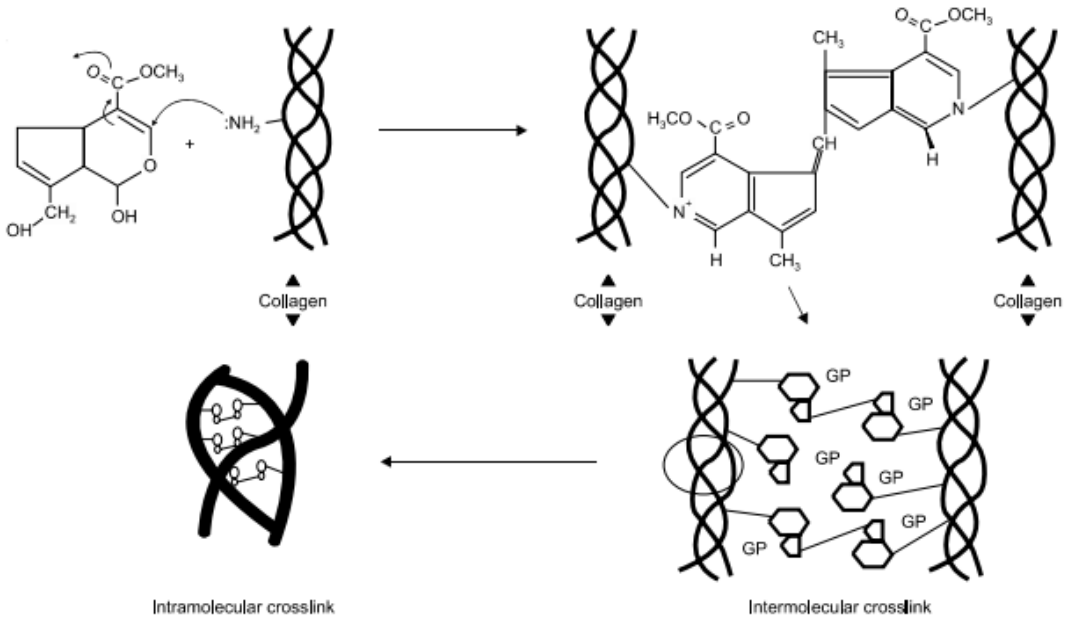

Note. Figure adapted from open access article (CC BY-NC 3.0)[52].

Genipin is a viable option for crosslinking due to its ability to interact and simultaneously react with amino groups that are located in collagen molecules which makes up the ECM. The binding of the genipin molecules to amino acids and proteins results leads to a spontaneous chemical reaction that produces blue coloration of the hydrogel [60]. Genipin is widely used due to its ability to withstand high temperatures, strong lights and pH fluctuations [52]. The most notable advantages of using genipin as a crosslinking agent include the increase in mechanical properties, resistance to enzyme degradation and the effects on physical properties such as heat resistance. In addition, numerous studies have shown that genipin has limited toxicity and holds crucial anti-inflammatory properties compared to other alternative chemical crosslinkers such as

www.manaraa.com

glutaraldehyde [52, 61, 62]. For this research, it is hypothesized that the previously described mechanism will result in the successful development of genipin crosslinked decellularized ECM hydrogels.

In addition to genipin crosslinking as a method to improve the limited structural stability of ECM hydrogels, other physical biomaterials have been investigated to further enhance the structural support provided to the 3D matrix. One of the most widely investigated physical biomaterials that are used to provide such support are nanofibers.

1.5 Introduction to Nanofibers

In the field of tissue engineering, fibers are typically classified based on their diameter, therefore fibers with diameters between 1µm and 1nm are considered to be nanofibers [63]. Nanofibers can then be further classified based on the orientation of the fibers located within the network. The two most prominent orientations that are observed with nanofiber fabrication are aligned nanofibers and randomly-oriented nanofibers. Typically, randomly-oriented nanofibers are collected on a grounded plate that is stationary and not rotating. The most distinctive feature of randomly-aligned nanofibers is the lack of unification and directionality (Figure 4: Right) [64].

In comparison, nanofibers that are predominantly parallel to each other are considered to be aligned (Figure 4: Left). Aligned nanofibers are typically generated using automated collectors such as rotating mandrels. Aligned nanofibers are advantageous for tissue and regenerative applications due to their ability to support and enhance cell attachment and growth in comparison to randomly oriented fibers [65, 66]. Furthermore, cells migration and growth have been shown to grow in parallel with the direction of the aligned fibers [67].

www.manaraa.com

Figure 4

Orientation of poly(lactide-co-glycolic acid) (PLGA) nanofibers

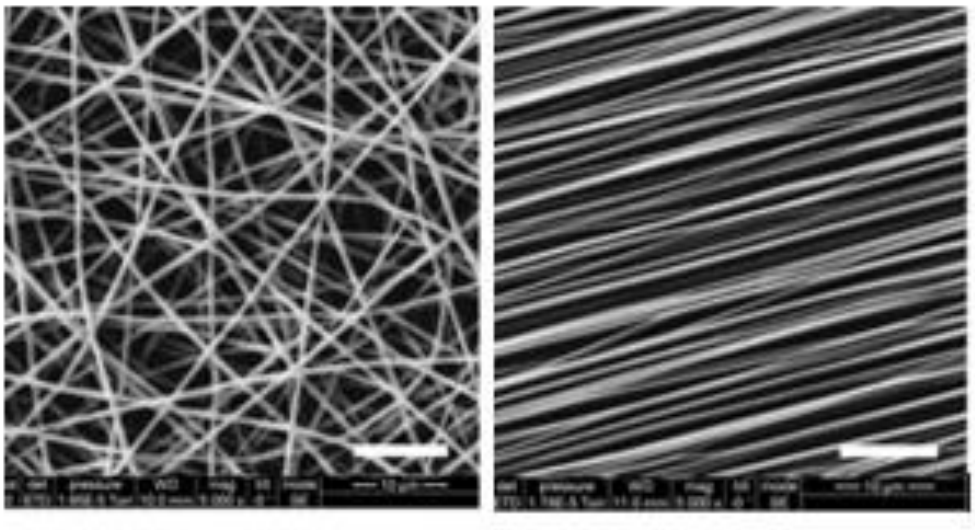

Note. Modified from Yu et. al. Left) Randomly orientated poly(lactide-co-glycolic acid) (PLGA) nanofibers. Right) Highly aligned PLGA nanofibers. Figure adapted from open access article (CC BY 4.0)[64].

1.5.1 Nanofiber Fabrication

Nanofibers are fabricated from a multitude of materials; however, the most commonly used materials are polymers such as poly(ethylene glycol) (PEG), poly(lactide-co-glycolic acid) (PLGA), poly(lactic acid) (PLA), polycaprolactone (PCL), polyacrylonitrile (PAN), polyethylene (PA) and poly(ethylene oxide) (PEO) [68]. These polymers are then dissolved in solutes such as dimethylformamide (DMF), dichloromethane (DCM), dimethyl sulfoxide (DMSO), chloroform and methanol at various ratios to form homogenous solutions. Once the polymer has completely dissolved

www.manaraa.com

in the respective solute and formed a homogenous solution, the polymer solution can be employed with a variety of methods to fabricate nanofibers.

Electrospinning is the most commonly studied and utilized method for fabricated nanofibers. Electrospinning is extremely versatile such that there is a wide variety of polymers that can be utilized to produce nanofibers. In addition, electrospinning is highly reliable and is capable of producing a larger amount of fibers at once compared to other methods of fabrication such as drawing where only one fiber is created at a time [69]. The process of fabricating electrospun nanofibers begins with a polymer being completely dissolved in a solvent of choice [70]. The polymer is loaded into a syringe and connected to a spinneret with tubing separating them. The syringe is held in place by a syringe pump and a high-voltage power supply is connected. Due to the large voltage applied to the needle, the formation of a Taylor cone occurs as the polymer is extracted from the needle. The jet that is sprayed out of the needle commonly exhibits a "whipping motion" which is due to instability of the solution [71, 72]. From this point, the nanofibers can be gathered below the electrospinner on a grounded collector.

A few different techniques are used for collecting electrospun nanofibers. Some of the most commonly employed methods are grounded collectors, rotating drums and parallel plate collectors. Grounded collecting plates are the most commonly used technique for collection resulting in randomly oriented mat of nanofibers. Rotating drum collectors, or simply, rotating mandrels are one of the leading methods for collecting aligned electrospun nanofibers. A rotating mandrel turns at continuously high speeds in order to collect fibers that are being ejected from the electrospinning jet above it. One of the key features that must be taken into consideration when collecting fibers with rotating mandrels

www.manaraa.com

is the rotation speed of the mandrel. Ideally, the mandrel should be rotating very quickly in order to ensure the fibers completely wrap around the mandrel and the orientation of the fibers are aligned [73]. When the rotating mandrel is set to less optimal speeds, fiber orientation transformed from mostly aligned strands to a more random orientation [74]. Parallel plate collection is another highly sought out method for collecting aligned nanofibers. Nanofibers used in this study were collected using a modified parallel plate technique where static plates are replaced by automated parallel tracks [75]. As the nanofibers move down the automated parallel tracks, they are deposited on a collecting rack and the final result is a mat of highly aligned nanofibers with well controlled fiber density.

Some of the most commonly utilized methods for producing nanofibers include drawing, templating, and self-assembly [76]. Drawing is technique that can be used to directly produce aligned nanofibers [77]. Drawing is a simple process in which a sharp tip such as micropipette comes into contact with droplet of polymer solution. Following contact, the sharp tip is pulled in the opposing direction, away from the polymer droplet which results in the formation of straight nanofibers. The drawing process can also be automated such that the polymer solution is pumped continuously through a glass micropipette while the pipette moves along the XYZ plane [78]. Drawing technique are advantageous due to method of fabrication being extremely feasible such that only a sharp tip or pipette tip is required. In addition, a wide variety of materials can be utilized. However, drawing is a time-intensive method of fabrication because only one fiber can be produced at a time. It has also been noted that fiber diameter is not always consistent which

www.manaraa.com

is not ideal for certain applications. Despite limitations, some recent advances have shown potential to scale up dip drawing [79].

Templating is a method that uses a specific mold or template to produce a given structure consisting of nanofibers. Template synthesis of nanofibers require the polymer solution to pass through the pores of the template which is a metal oxide membrane. In order for extrusion of the polymer to form nanofibers, the polymer must pass through the nanopores under a constant water pressure on the other side of the membrane [76]. Following nanofiber formation, the fibers can be collected by breaking apart the mold or by other means that involve physical or mechanical movements [80]. Li *et. al* demonstrated that this method could be successfully employed with an anodic aluminum membrane in order to obtain polyethylene (PE) nanofibers [81]. Some of the key advantages of the template synthesis method are the ability of the fiber diameter and length to be controlled [76, 82]. Furthermore, fabrication of different molds or templates were varying diameters can in terms produce nanofibers with distinctly different diameters.

Self-assembly is an additional method that can produce nanofibers through the organization peptide molecules into random patterns and networks. The mechanism of nanofiber formation is linked to the intramolecular, non-covalent forces that bring the molecules together [82]. Furthermore, self-assembled nanofibers can be tuned for specific applications based on the amino acids located within the peptide chain which determine their respective biological and chemical properties [83, 84]. One of the major advantages of self-assembling nanofibers is the resulting 3D porous structure that can be utilized for direct injections for *in vivo* applications[82]. Numerous *in vivo* studies investigating self-assembling nanofibers and the corresponding network that are formed have been

www.manaraa.com

conducted. The studies have demonstrated that the networks formed via self-assembly are capable of enhancing cell attachment and infiltration [85].

Electrospinning is one of the most commonly utilized techniques for producing both aligned and randomly oriented nanofibers due to its low cost and high yield [82]. For this reason, this research chose to fabricate highly aligned electrospun nanofibers. In addition, electrospinners are very feasible in terms of set-up and offer numerous methods to alter or tune nanofiber characteristics such as fiber diameter and the internal microstructure of the nanofibers. However, electrospinning often utilizes solvents such as chloroform, dimethyl formaldehyde (DMF) and methanol which are extremely toxic to cells [86]. Furthermore, numerous studies have shown that electrospun nanofiber structures exhibit substantially less cell infiltration into the center of the scaffold [87]. Therefore, this research aims to improve and promote cell infiltration by developing a hydrogel nanofiber composite that will add space between the fibers.

1.5.2 Applications of Nanofibers

Nanofibers are commonly employed in controlled drug delivery systems as a method of encapsulation of crucial therapeutics such as tetracycline hydrochloride for the treatment of periodontal disease [88]. Furthermore, PLGA nanofibers were fabrications for the delivery of antibiotics as demonstrated by Kim *et. al.*[89]. The unique characteristics of nanofiber structure such as their ability to carry and release therapeutics at tunable release rates makes them a suitable option for drug delivery systems.

In addition to controlled drug delivery systems, nanofibers are also applicable for developing biosensors and smart clothing. One of the main factors taken into consideration for designing wearable electronics and biosensors is that they must be flexible and easily

www.manaraa.com

stretchable [90]. Furthermore, electrical conductivity is a highly sought-after feature of biosensors and smart clothing. Reich et. al described a nanofiber composite consisting of PCL, PAN and nonwoven silver nanowires (AgNW) that provided substantial electrical conductivity properties [91]. Additionally, the amount of electrical conductivity was unrelated to the deformation brought on by bending of the structure. This is a critical finding such that wearable technology must be able to function at extreme angles and maintain flexibility and stretchability.

Furthermore, nanofibers are often fabricated for tissue and regenerative engineering applications. This is mainly due to the ability of nanofibers to promote cell growth and adhesion due to high surface to volume ratio of the fibers [92]. The 3D network that the nanofibers produce allow cells to successfully function and grow in an environment that closely mimics the natural *in vivo* environment [93, 94]. The highly aligned orientation of nanofibers are most advantageous when it comes to promoting cell attachment, alignment and elongation which is crucial for regeneration of tissues such as cartilage, tendon and ligaments.

1.6 Overview of Project Goals and Objectives

The goal of this research is to develop repeatable methods to fabricate bovine tendon derived ECM hydrogels that can have translational applications in tissue and regenerative engineering. In addition, this research aims to improve upon the mechanical limitations and stability of ECM hydrogels by incorporating genipin, a natural crosslinker derived from plants. Furthermore, PCL electrospun nanofibers will be fabricated and dipped in dECM hydrogel solutions containing MSCs with no genipin or 1mM genipin. The goal of dip coating aligned PCL nanofibers in dECM hydrogel solutions was to

www.manaraa.com

investigate if the aligned nanofibers could promote cell alignment in the direction of the fibers and therefore replicate the alignment of ECM found in native tendon [95]. It is hypothesized that the addition of the chemical crosslinking agent, genipin will enhance the mechanical properties of the ECM hydrogels without the inducing cytotoxic side effects linked to alternative crosslinking agents such as glutaraldehyde. It is also hypothesized that the incorporating of electrospun PCL nanofibers within the hydrogel network will allow for enhanced cell growth and proliferation as well as cell alignment in the direction of the nanofibers.

The bovine derived dECM hydrogels developed in this research will be investigated for indications of cytotoxic effects on mammalian mesenchymal stem cells. In order to determine the success of these goals, dECM hydrogels will be evaluated *in vitro* in terms of their mechanical properties, degradation characteristics, and biocompatibility (with and without the addition of electrospun nanofibers). Chapter 2 describes in detail numerous well-thought-out methods employed to fabricate and characterize the dECM hydrogels developed in this research.

www.manaraa.com

Chapter 2

Methods

2.1 Introduction

Throughout the duration of this research, numerous methods were utilized in order to formulate and characterize the hydrogels developed. In this chapter, a brief overview of the methods employed will be discussed. Some of the characterization methods that will be discussed include hydrogel fabrication, genipin formulations, enzymatic degradation, rheology, spectrophotometry and cell culture techniques.

2.2 Hydrogel Fabrication

2.2.1 Tendon Sterilization and Decellularization

Fresh bovine tendon (Bringhurst Meats, Berlin, New Jersey) was used to create ECM hydrogels. The bovine tendon was used as needed and the remainder was kept at -20°C. The bovine tendon was thawed in deionized water and a scalpel was used to remove excess fat and muscle in order to isolate the tendon. Once the tendon was isolated, it was cut into small cubes. Established from adapted protocols, tendon samples were subjected to constant agitation on a stir plate (300 RPM) and treated with a 10% Triton X-100 (Millipore Sigma, St. Louis, MO) solution for 24 hours at 37°C [96]. Following the Triton X1-00 exposure, the decellularized ECM (dECM) was thoroughly washed in PBS for 24 hours followed by a 24-hour diH_2O washed to remove any remaining cellular material and excess solvent. After the PBS/diH_2O wash, the dECM was snap frozen using liquid nitrogen. The sample was lyophilized overnight and the following day the sample was

www.manaraa.com

ground up in a generic coffee grinder (Krups, USA) to create a powder like substance that was stored in the freezer at -20°C until needed.

2.2.2 Digestion and Solubilization

Adapted from previous techniques**,** dECM was mixed with 1 mg ml^{-1} pepsin (Millipore-Sigma, Milwaukee, WI) in 0.01 N HCL which resulted in an overall 10 mg per ml dECM solution [97]. The solution was then set on a stir plate for 72 hours, or until the decellularized matrix was completely dissolved. The pepsin digest solution was then neutralized to a pH to 7.4. Neutralization of the solution was achieved adding 0.01 N NaOH at one-tenth of the volume of pre-gel solution and adding one ninth the volume of 10× PBS. Neutralization was conducted on ice or at 4°C. [98]. Gelation of ECM hydrogels occurred after approximately 8 minutes following a temperature raise from at 4°C to 37°C. Characterization of 3,6 and 8 mg/ml hydrogels revealed much lower structural integrity and stiffness in 3 and 6 mg/ml hydrogels. This lead to decreased feasibility of use for further genipin characterization. For this reason, all future experiments involving genipin crosslinking utilized 8 mg/ml ECM hydrogels.

2.3 Quantification of Cellular Content

Hydrogel pre-gel solutions containing non-decellularized ECM (bECM) and dECM were creating using the previously mentioned protocol. In brief, bECM was snap frozen using liquid nitrogen and ground into a fine, powder-like substance. The sample was then lyophilized overnight. A hydrogel pre-gel solution was then prepared using identical methods as mentioned before. The same protocol was followed to prepare a dECM solution, however this solution was treated with a chemical detergent, Triton X-100. Adhering to the supplier protocol, DNA content was measured using an Accublue® Broad

www.manaraa.com

Range dsDNA Quantitation Kit (Biotium, United States). A standard curve was produced with the known DNA concentrations ranging from 0 to 200 ng/uL. A M3 Spectramax (Molecular Devices, USA) plate reader was used to read and record all plate values.

2.4 Analysis of Genipin Crosslinking

2.4.1 Genipin Crosslinking of dECM Hydrogels

Genipin was dissolved in Dimethyl Sulfoxide to produce a 0.5%w/v solution [54, 56]. Three different concentrations of genipin were tested in the ECM hydrogels, 0.1, 0.5 and 1 mM, respectively. In addition, ECM hydrogels containing no genipin were utilized to serve as a control. The genipin crosslinker was added to ECM pre-gel solution prior to polymerization. Noticeable crosslinking was observed after two hours by visualization of blue coloration of the hydrogel. ECM hydrogels were exposed to genipin for 24 hours in order to insure complete crosslinking had occurred. Following the 24 hours crosslinking period, the dECM hydrogels were washed trice in PBS to remove any remaining, unreacted crosslinker.

2.5 Rheological Characterization of dECM Hydrogels

2.5.1 Temperature Ramps

A temperature ramp and time sweep were conducted simultaneously to determine the gelation kinetics of the genipin crosslinked ECM hydrogels. This method was also used to evaluate the possible long-term stability of the ECM hydrogels. To determine the gelation kinetics of ECM hydrogels, 3, 6 and 8 mg/ml ECM hydrogels (n=3 for all concentrations) were loaded onto a Discovery HR-1 Hybrid Rheometer (TA Instruments, USA) and subjected to 0.5% strain and a frequency of 1 Hz as the temperature increased from 10°C to 37°C. The starting temperature was set to 10° C rather than of 4°C due to the

www.manaraa.com

appearance of moderate condensation which resulted in slippage of the hydrogels. A 20 mm 1° cone and plate set up was used to test the hydrogels with a gap of 30 µm. In addition, a custom-made humidity chamber was employed to prevent hydrogel evaporation. The humidity chamber was manufactured using a modified petri dish that fit around the dimensions of the rheometer attachment. Enough PBS was pipetted onto the modified petri dish to provide complete coverage. The temperature ramp was set to run for 30 minutes in order to observe the critical point at which G'(storage modulus) crosses over G''(loss modulus).

2.5.2 Oscillatory Strain Sweeps

Strain sweeps are critical for characterizing complex systems such as hydrogels. The outputs of a strain sweep will determine the linear-viscoelastic region of the material in question, in this case it is naturally derived ECM hydrogels. The modulus of hydrogels are independent of applied strain to up to a certain point at which the hydrogel transforms from a linear viscoelastic material to a non-linear material [99]. This point is known as the critical strain and once the material crosses the critical strain, the material breaks. In order to determine the linear-viscoelastic region of the bovine derived ECM hydrogels in this research, 3, 6 and 8 mg/ml hydrogels (n=3 for all conditions) were subjected to oscillatory strain sweeps. Immediately following the temperature ramp, the hydrogels were subjected to an oscillatory strain sweep at a constant frequency (1 Hz) and temperature (37°C). The strain amplitude progressively increased in the range of 0.01 to 150% strain to determine the linearity of the hydrogel. Some experiments were terminated before 150% strain could be achieved due to the critical strain being reached prior to 150%.

www.manaraa.com

2.5.3 Oscillatory Frequency Sweeps

Hydrogels will transform from a mainly liquid state into a mostly solid like material with increasing frequency [100]. In order to determine the complex viscosity, an oscillatory frequency sweep within the linear viscoelastic region was conducted on ECM hydrogels. Fully polymerized hydrogels with 3, 6 and 8 mg/ml ECM (Nn=6 for each concentration) concentration were loaded onto the rheometer. In addition, 8 mg/ml ECM hydrogels exposed to genipin (0.1, 0.5, and 1 mM) (n=6 for each condition) were also subjected to frequency sweeps. All gels that exceeded the volume required for the 20 mm plate were trimmed prior to running the experiment. The hydrogels were put under a shear stress of 20 Pa as the frequency ranged from 0.01 to 100 Hz [101]. The amplitude and temperature were kept constant during the frequency sweep.

2.5.4 Oscillatory Stress Sweeps

It is known that materials such as hydrogels will resist flow unless a critical threshold, known as yield stress, is crossed [102, 103]. A material that sustains a stress value below the critical threshold will maintain a solid-like form, however once the material crosses the yield stress the resistance to flow decreases and the material takes on liquid-like properties. In order to analyze the yield behavior of uncrosslinked 3,6 and 8 mg/ml dECM hydrogels (N=3 for all concentrations), an oscillatory stress sweep was conducted. The frequency and temperature were held constant for the duration of the test (0.159 Hz and 37°C, respectively). To determine the critical stress point in the linear viscoelastic region the stress applied to all ECM hydrogels ranged from 0.1 to 50 Pa. In some cases, stress sweeps were terminated before 50 Pa could be reached due to differences in the yield stress range for 3,6 and 8 mg/ml dECM hydrogels.

www.manaraa.com

2.6 Enzymatic Degradation

ECM hydrogels (8 mg/ml) crosslinked without genipin (0 mM) and with genipin (0, 0.1, 0.5, and 1 mM) were formed in microcentrifuge tubes and allowed to form overnight to ensure maximum crosslinking. Following complete crosslinking, the hydrogels were washed three times in PBS for 20 minutes to remove any unreacted genipin. Adapted from previous techniques, following the 20-minute washes, the gels were exposed to collagenase (0.1wt%) in PBS with 0.9 mM $CaCl_2$ for 30, 60, 90 or 120 minutes [56]. Hydrogel controls containing no genipin were exposed to only PBS for the same amounts of time. The microcentrifuge tubes were set on a rocker at 80 rpm to ensure the hydrogels were adequately exposed to the collagenase for each time point. After 30, 60, 90, or 120 minutes, the collagenase was aspirated out of the tubes and the gels were washed in triplicate in PBS to remove any residual collagenase. The PBS washes were incorporate to account for the possible errors in mass values due to the presence of salt. The hydrogels were then lyophilized overnight and weighed. The dry weights of the ECM hydrogels were recorded as % Mass Loss (Equation 1) and presented as % Mass Remaining (Equation 2). Mass Loss was calculated as the ratio of the dry weight of the collagenase exposed hydrogels (M_f) versus PBS exposed control hydrogels at the same time point (M_i). All degradation studies were replicated in three times for each of the four conditions at 30, 60, 90 and 120 minutes respectively.

$$\% \text{ Mass Loss} = \frac{M_i - M_f}{M_i} * 100\% \quad (1)$$

$$\% \text{ Mass Remaining} = 100\% - \% \text{ Mass Loss} \quad (2)$$

www.manaraa.com

2.7 In Vitro Biocompatibility Test

In order to assess the biocompatibility and cytotoxicity of the dECM hydrogels fabricated in this research, two in-vitro cell-based assays were conducted. Prior to experimentation, all hydrogels were formed in a sterile hood using sterile techniques. In addition, all materials being utilized were sterilized by UV light for approximately 30 minutes. Mammalian mesenchymal stem cells (MSCs) (Lonza) were thawed at passage 2-3 and cultured on tissue culture plates until confluency in 10% media containing Alpha MEM (AMEM,(Lonza), fetal bovine serum (FBS,Gibco) and penicillin-streptomycin (Gibco).

2.7.1 2D Cell Studies

For 2D *in vitro* cell studies, 8 mg/ml hydrogels crosslinked with genipin (0.1, 0.5, and 1mM) were formed in 24-well plates. Hydrogels that were not exposed to genipin were also developed to serve as a control. The hydrogels were allowed to fully polymerize and crosslink over a 24-hour time period. Prior to cell seeding, the hydrogels were all washed 5 times with PBS to remove any excess crosslinking agent. For all 2D cell culture work, MSCs were seeded at a density of 3×10^3 cells/cm^2 directly on top of the polymerized hydrogels in 24-well plate in 500 ul volume per well.

2.7.2 3D Cell Studies

For 3D cell seeding, MSCs were resuspended directly into the 8 mg/ml hydrogel solution at a density at 1×10^6 cells/mL prior to polymerization. The hydrogels were crosslinked similarly to 2D hydrogels, with 0.1, 0.5 and 1 mM genipin or no genipin (control). dECM hydrogels with resuspended MSCs were formed in 24 well plates. 500 ul

www.manaraa.com

of the hydrogel solution containing MSCs was dispensed per well in a 24 well-plate respectively.

2.7.3 Live/Dead Assay

In order to obtain qualitative data regarding the cytotoxic effects of genipin crosslinking on dECM hydrogels, 2D and 3D hydrogels containing 0 (control), 0.1, 0.5 and 1 mM genipin were formed in 10 mm circular PDMS molds in triplicate for each condition. All 2D and 3D hydrogels were assessed using a Live/Dead (Invitrogen, Thomas Scientific) assay after 1, 3 and 7 days. 2D hydrogels were exposed to the Live/Dead stain and incubated at 37°C, 5% CO_2 for 30 minutes on day 1, 3 and 7. 3D hydrogels were exposed under the same conditions expect for 1 hour instead of 30 minutes. Following exposure to the Live/Dead stain, the 2D and 3D hydrogels in PDMS molds were transferred to a glass coverslip and analyzed immediately using a Nikon A-1 confocal scanning microscope. All Live/Dead assays for conducted on 2D and 3D hydrogels were replicated in triplicate, three independent experiments observing all genipin concentrations (0,0.1,0.5 and 1mM) at 1, 3 and 7 days.

2.7.4 Alamar Blue Assay

In addition to the qualitative assay, a quantitative analysis to determine cell viability in 2D and 3D hydrogels was assessed using Alamar Blue to confirm the initial findings observed in the Live/Dead Assay. For all Alamar Blue experiments conducted, 2D and 3D hydrogels were formed with 0,0.1, 0.5 or 1mM genipin in 24-well plates. Each hydrogel condition for Alamar Blue assessment was replicated in triplicate. At day 1, 3 and 7 respectively, the growth medium in each well was removed and replaced with 10% Alamar

www.manaraa.com

blue reagent and incubated for 4 hours at 37°C, 5% CO_2. Following exposure, 50 uL aliquots were taken in quadruplicate from each well and transferred into a 96 well. The fluorescence was measured at 560 nm (excitation) and 590 nm (emission) using a M3 Spectramax (Molecular Devices, USA). An alamar blue standard curved was derived in order to quantify the amount of cells/well. Furthermore, alamar Blue assays for 2D and 3D hydrogels were conducted in quadruplicate, to be specific, four independent experiments observing 0, 0.1, 0.5 and 1mM genipin crosslinking at 1, 3 and 7 days.

2.8 ECM Nanofiber Composite Structure Fabrication

Polycaprolactone (PCL, Mn=115 kDa, Sigma) was dissolved in a 3:1 dichloromethane/dimethyl formaldehyde ratio (Sigma) at 18% w/v. In order to observe the fiber layers, a fluorescent red lipophilic indocarbocyanine dye, DiI (Invitrogen, Thomas Scientific) was added to the PCL solution at 0.1 wt%[104]. Nanofibers were created by feeding the PCL solution through a 24-gauge needle at 2.0 ml/min with an applied voltage of 10 kV. Aligned nanofibers were fabricated using previously described methods where automated parallel tracks were used to draw nanofibers down the track (Figure A1)[105]. The fibers were then collected on a rack sitting below the tracks. The aligned nanofibers were in numerous sessions consisting of 20-minute intervals. Following collection, stainless steel rings with a 1-inch diameter were adhered to the aligned nanofibers with silicone adhesive and individually cut out.

2.8.1 Sterilization of PCL Nanofibers

Framed nanofibers of the previously described dimensions were sterilized in 1 N hydrochloric acid (HCL). The framed nanofibers were placed in a 6-well plate and soaked in 3mL of 1 N HCL for 30-45 minutes at room temperature. Following sterilization, framed

www.manaraa.com

nanofibers were washed trice in PBS. After the three PBS washes, the nanofibers were submerged in fresh PBS and the pH was checked to ensure all excess HCL had been removed. The sterilized fibers in 6-well plates were stored in PBS at 4°C until further use.

2.8.2 Dip Coating PCL Nanofibers with ECM-Cell Solution

For dip coating techniques, passage 1-3 mammalian MSCs were prepared at ~80% confluency from 100 mm tissue culture plates. The cell pellet obtained from the tissue culture plate was resuspended in one of two ECM solutions, both at a density of 1.5 x 10^6 cells/ mL. The two solutions were as follows, a dECM hydrogel solution containing 1 mM genipin concentration or a dECM hydrogel solution containing no genipin. Previously sterilized framed nanofibers were dipped in one of the two ECM solutions in a way that ensured all nanofibers were completely coated in the ECM solutions containing MSCs. The dipped nanofibers were placed in a tissue culture plate (TCP) and allowed to polymerize for 30 minutes to 1 hour. Following this, the dipped nanofibers were completely immersed in AMEM containing 10% FBS. The ECM dipped nanofiber frames containing no genipin and 1 mM genipin were incubated at 37°C, 5% CO_2 for 1, 3 and 7 days until cell viability assessment via Live/Dead assay. Due to time constraints, ECM dipped nanofiber frames with both genipin conditions (0 and 1mM) were investigated at n=1.

www.manaraa.com

Chapter 3

Results and Discussion

3.1 Synthesis of dECM Hydrogels

In this research, a repeatable protocol for formulating bovine derived ECM hydrogels at 3, 6 and 8 mg/ml were all successfully established (Figure 6). All hydrogels polymerized following neutralization of the ECM solution and incubation at 37°C. Hydrogels formed at 3 and 6 mg/ml visually exhibited less structural stability and were more prone to breakage during handling and transferring. For this reason, crosslinking of the hydrogels with genipin was only conducted on 8 mg/ml dECM hydrogels for rheological characterization, enzymatic degradation, and cell viability. As previously mentioned, 8 mg/ml ECM hydrogels were genipin crosslinked at three different concentrations, 0.1, 0.5 and 1mM genipin respectively (Figure 6E-G). Genipin crosslinking of the network was visibly apparent after approximately 2 hours via color change (Figure A2) .

All hydrogels fabricated in this research conformed to the shape of the mold or container they were fabricated in. For example, hydrogels formed in 24-well plates exhibited flat, circular morphology whereas hydrogels formed in microcentrifuge tubes took on a more elongated, tube like structure. Interestingly, when hydrogels formed in microcentrifuge tubes were removed and places on a flat surface, they did not maintain the long, elongated structure. Instead, they flattened out and spread into a circular morphology.

www.manaraa.com

Figure 5

The overall process of forming genipin crosslinked dECM hydrogels

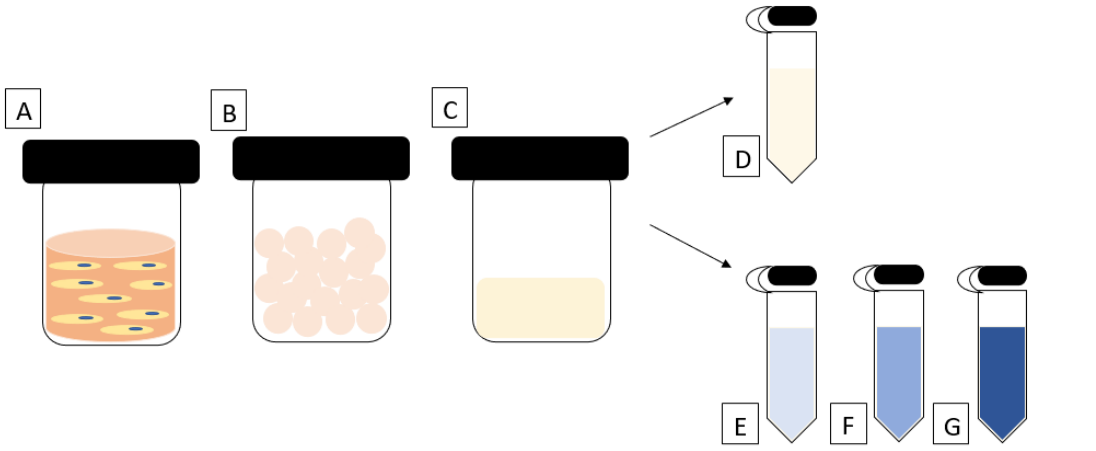

Note. A) Frozen bovine derived tendon. B) Decellularized and lyophilized dECM powder. C) ECM powder digestion and solubilization. D) Uncrosslinked dECM hydrogels. E) 0.1 mM genipin crosslinked dECM hydrogel. F) 0.5 mM genipin crosslinked dECM hydrogel. G) 1 mM genipin crosslinked dECM hydrogel.

3.2 Quantification of Cellular Content

Successful decellularization of bECM conformed to the previously established threshold that the samples should contain less than 50 ng of double standard DNA (dsDNA). Quantification of dsDNA content indicated that the quantity of DNA present in both bECM and dECM samples were both much lower than the critical value of 50 ng dsDNA/ mg ECM dry weight commonly reported in literature (Figure 8) [18, 106]. More specifically, the cellular content of the bECM and dECM materials were found to be 3.75±0.17 and 2.86±0.11 ng dsDNA/ mg ECM dry weight respectively. Significance was identified between the bECM and dECM samples which indicate a substantial difference

www.manaraa.com

in cellular content therefore validating the method of decellularization utilized in this research. It is worth noting, that tendon tissue typically containing low DNA content and the results obtained in this research are very similar to that previously reported in literature[96].

3.3 Mechanical Properties of dECM Hydrogels

3.3.1 Gelation Kinetics Results

In rheology characterization, the storage modulus (G') of a material is a measure of its stored, elastic contributions whereas the loss modulus (G'') is a measure of its viscous energy [107]. Polymerization of the hydrogel network is denoted by the critical cross-over point in which the storage modulus (G') crosses over the loss modulus (G''). The crossover point of 3,6 and 8 mg/ml dECM hydrogels all occur at approximately 250 seconds (Figures A3-A5). In addition, the phase angle can also serve as an indicator for polymerization. Prior to gelation, the phase angle of 3,6 and 8 mg/ml dECM hydrogels were all within the range of 80-90°, indicative of highly viscous behavior. Following the cross-over point, the phase angle sharply decreased within the range of 10-25°, indicative of the hydrogel transitioning from a more viscous phase to a more elastic state. Confirmation of hydrogel formation was further verified by visual observation after the parallel plate was lifted following the completion of the temperature ramp. The maximum storage modulus was determined by observing the point at which the storage modulus no longer increased and instead began to plateau. The maximum storage modulus for 3, 6 and 8 mg/ml dECM hydrogels were 35.87±13.98 Pa, 123.19±56.60 Pa and 315.10±49.30 Pa respectively (Figure 12). The data suggests a direct relationship between the ECM concentration and

www.manaraa.com

the maximum storage modulus such that as the concentration of ECM increased, the maximum storage modulus also increased.

Figure 6

Assessment of cellular content to confirm decellularization of the bovine tendon

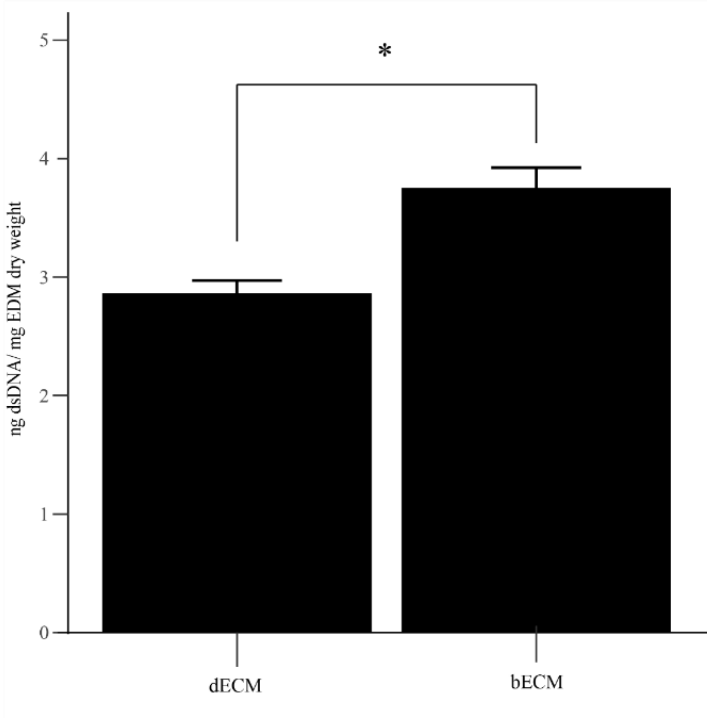

Note. An Accublue Broad Range dsDNA quantification kit was utilized to assess the cellular content of dECM and bECM. Data is representative of the Mean ± SEM of n=3. Significance is indicated by the star above the group ($p < 0.05$).

www.manaraa.com

Figure 7

Maximum storage modulus (G') obtained from 3, 6 and 8 mg/ml dECM hydrogels

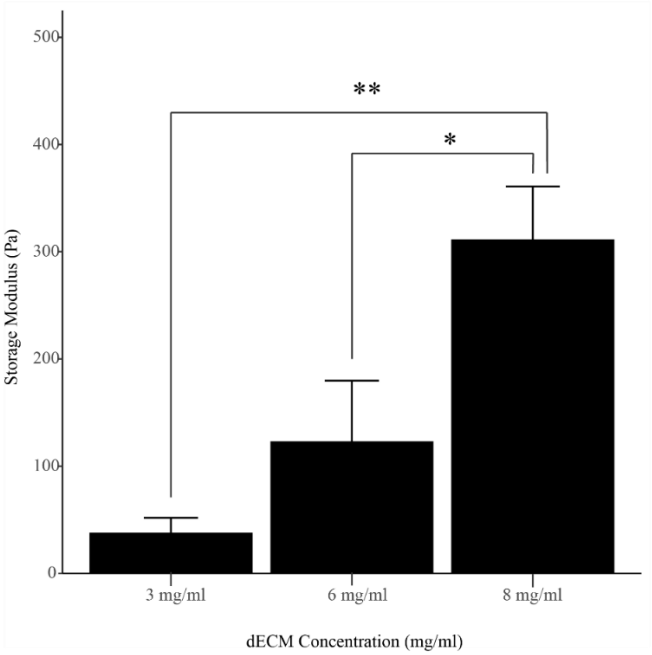

Note. These results were obtained via gelation kinetics. Data is representative of the Mean ± SEM where n=3 for each dECM concentration. *, Significance between 6 and 8 mg/ml dECM hydrogel G' ($p < 0.05$): **, Significance between 3 and 8 mg/ml dECM hydrogel G' ($p < 0.001$).

3.3.2 Strain Sweep Results

Strain sweeps were conducted on dECM hydrogels immediately following temperature ramps. Hydrogels at concentration of 3, 6 and 8 mg/ml were subjected to strain sweeps in order to determine the linear-viscoelastic region. The findings from this research confirm previous findings that hydrogel mechanics are independent of the applied strain up until a critical point. 3 mg/ml hydrogels peaked at a storage modulus of 8.27 Pa ± 0.42 and a strain of 25.92% (Figure 13A). 6 mg/ml had a max modulus of 123 Pa ± 83.85 with

www.manaraa.com

a critical strain of 7.61% (Figure 13B) and 8 mg/ml hydrogels achieved a storage modulus of 285. 04 Pa ± 120.21 at a strain of 6.12% (Figure 13C). After the hydrogels reached their respective critical strains, their characteristic behavior transformed from a more elastic material to a non-linear viscous material. As the strain applied to the hydrogel increases, the hydrogel has less time to relax and return to its original state. Furthermore, as the strain increases the twist-like motion applied to the hydrogel simultaneously increases which results in the breakage of bonds within the hydrogel. Therefore, the decreased relaxation time and bond breakage results in the sharp decline in the storage modulus. The critical stress was also confirmed by observing a shift in the phase angle of the hydrogels. Before the critical strain was reached, all hydrogels maintained a phase angle in the range of 10-25°, however after the critical strain the phase angle increased sharply, indicative of the hydrogel transitioning from a more solid like structure into a more viscous material.

www.manaraa.com

Figure 8

Strain amplitude sweeps of 3, 6 and 8 mg/ml dECM hydrogels

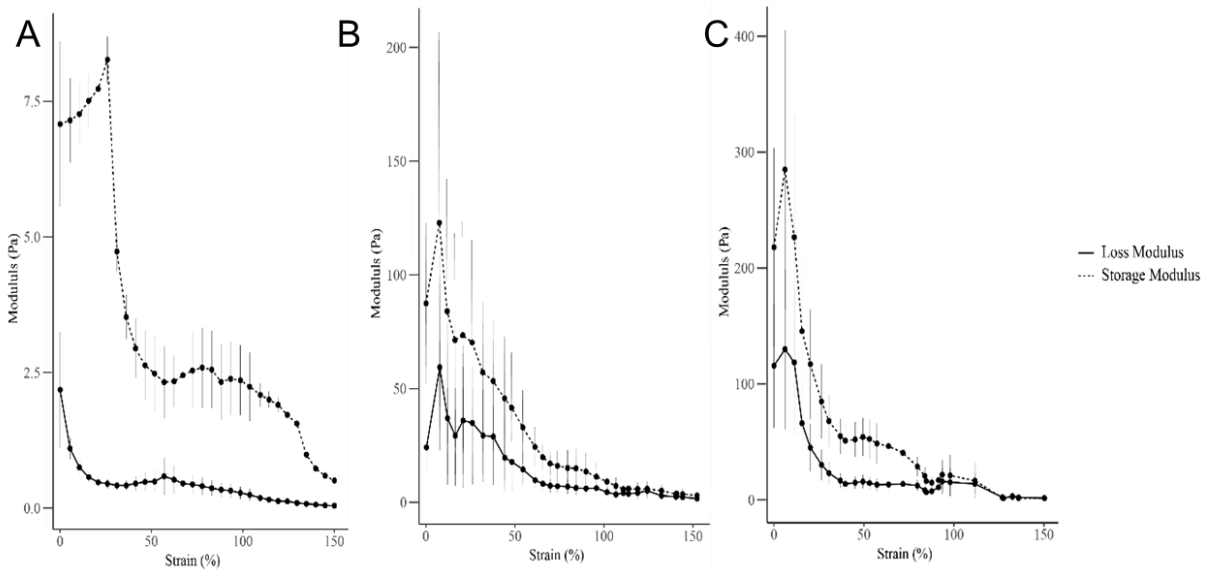

Note. Strain sweeps were conducted at a constant frequency (1 Hz). Both storage modulus (G') and loss modulus (G") were observed as the hydrogels were subjected to strain ranging from 0.1 to 150%. (**A**) 3 mg/ml dECM hydrogel, (**B**) 6 mg/ml dECM hydrogel, (**C**) 8 mg/ml dECM hydrogel. Data is represented at Mean ± SEM for n=3.

3.3.3 Frequency Sweep Results

Hydrogels transform from a mostly liquid material into a primarily solid like structure with increasing frequencies as indicated by an increase in the storage modulus. Therefore as the frequency increases, the hydrogel behavior is associated less with the viscous behavior and increasing related to the elastic behavior.

In this research, preformed hydrogels (n=6 for all concentrations) subjected to a frequency sweep in range of 0.1 Hz to 100 Hz displayed a consistent trend in regard to the concentration of ECM within the hydrogels and their respective storage moduli. As the

www.manaraa.com

concentration within the dECM hydrogels increased, the storage moduli also increased. The max storage modulus obtained from 3 mg/ml dECM hydrogels was 322.40 Pa ± 43.60 (Figure 14A) compared to 392.57 ± 6.15 Pa for 6 mg/ml (Figure 14B) and 407.54 ± 69.53 Pa for 8 mg/ml dECM hydrogel (Figure 14C). Furthermore, frequency independent behavior of the 3, 6 and 8 mg/ml dECM hydrogels can be observed when the complex modulus of the hydrogel is in sync with the storage modulus (where G*=G'). The storage modulus of 8 mg/ml dECM hydrogels that are independent of the applied frequency further substantiate the claim that the hydrogels have completely polymerized and have formed a solid-like network.

In addition, a positive relationship was observed between the genipin concentrations (0.1, 0.5, and 1 mM) used to crosslink 8 mg/ml dECM hydrogels and their storage moduli. As the concentration of genipin within the preformed 8 mg/ml dECM hydrogels increased, the storage modulus at the each genipin concentration (0.1, 0.5, 1 mM) also increased (Figure 15). The maximum storage modulus obtained from 0.1 mM genipin crosslinked 8 mg/ml dECM hydrogels was 333.69 ± 23.82 Pa 0.5 mM genipin crosslinked hydrogels maintained a max storage modulus of 452.57 ± 9.71 Pa and 1 mM genipin crosslinked hydrogels exhibited a max storage modulus of 521.74 ± 16.22 Pa. In comparison, the maximum storage modulus obtained from an 8 mg/ml dECM hydrogel with 0 mM genipin was 315.10 ± 9.91 Pa.

The direct relationship between ECM and storage modulus as well as ECM and genipin concentration indicates that there is potential for the mechanical properties of dECM hydrogels to be altered and tuned for specific applications.

www.manaraa.com

Figure 9

Frequency sweeps conducted on preformed 3,6 and 8 mg/ml dECM hydrogels

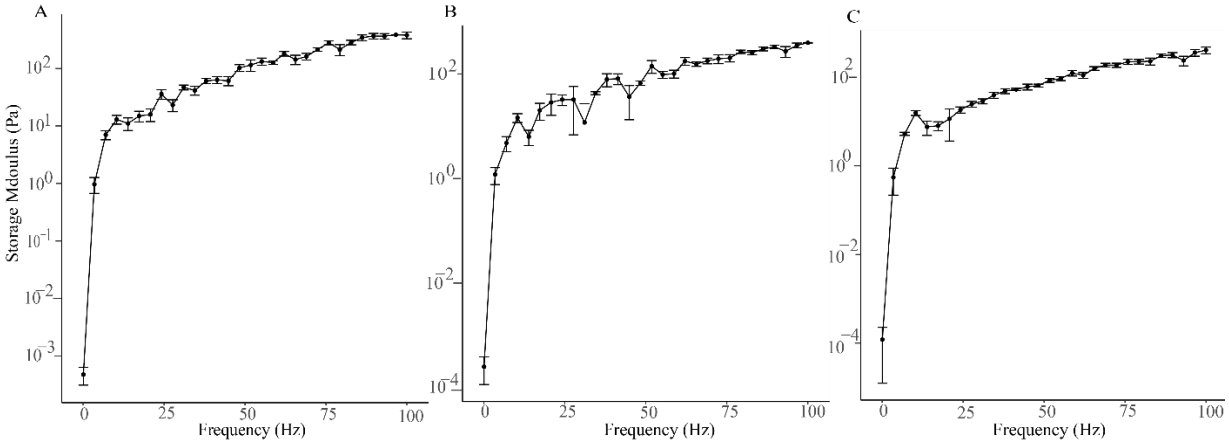

Note. Frequency ranged from 0.1 to 100 Hz at a constant stress of 20Pa. (**A**) 3mg/ml dECM hydrogel, (**B**) 6mg/ml dECM hydrogel, (**C**) 8mg/ml dECM hydrogel. Data is represented as Mean ± SEM for n=6.

www.manaraa.com

Figure 10

The effects of genipin crosslinking on preformed 8mg/ml dECM hydrogels

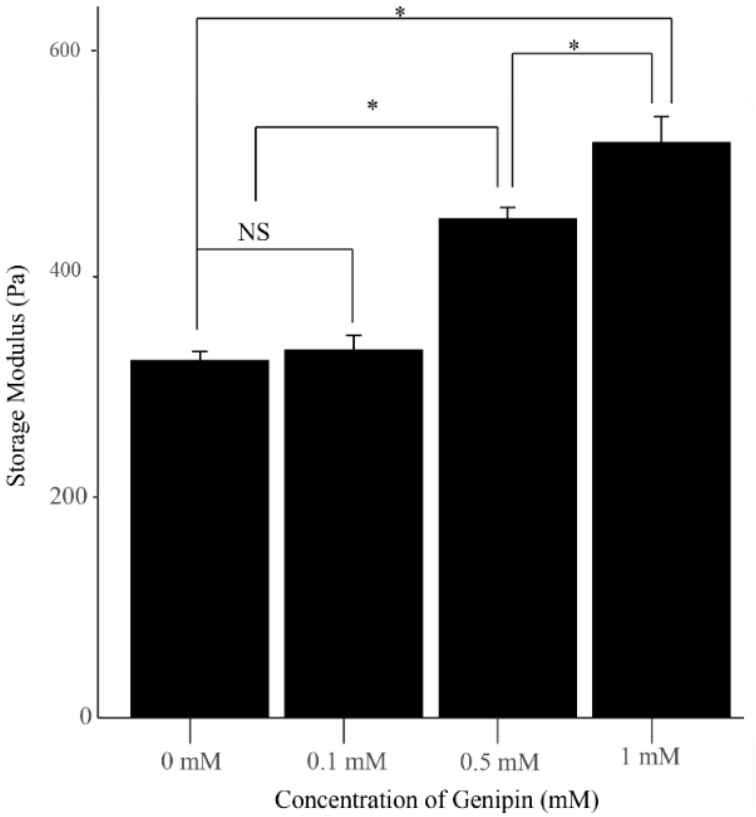

Note. Concentrations of genipin utilized are 0.1 mM, 0.5 mM and 1mM. Data is represented as Mean ± SEM for n=3. *, Significance between the group connected by solid line ($p < 0.001$). There was a significant different in the storage modulus of all group except for 0 mM and 0.1 mM genipin.

3.3.4 Stress Sweep Results

Immediately following gelation, hydrogels at all concentrations were subjected to stress sweeps until the yield stress was reached and the hydrogel began to break. All hydrogels examined were independent of stress up until a certain point. The resulting yield stress for 3 mg/ml dECM hydrogels was approximately 0.81± 0.01 Pa (Figure 16A). In

www.manaraa.com

comparison 6 mg/ml dECM hydrogel yield stress was 2.16 ± 0.11 Pa (Figure 16B) and 0.80± 1.14 Pa for 8 mg/ml dECM hydrogels (Figure 16C). These results indicate that 6 mg/ml hydrogels have the highest yield stress and are able to withstand the most applied stress, however it is the 8 mg/ml hydrogels that have the most structural stability as determined by the storage modulus. The respective moduli at the yield stress points for 3, 6 and 8 mg/ml dECM hydrogels were 12.575 ± 1.90 Pa, 105.40± 32.80 Pa, and 230.268 ± 22.68 Pa respectively. Following the stress sweep, the hydrogels were visually observed for changes in their physical appearance. After hydrogels had reached their respectively yield points, the physical structure transitioned from a more elastic, solid like structure to a more viscous material. This transition was evident due to the hydrogel separating into numerous chunks instead of remaining one solid structure.

www.manaraa.com

Figure 11

Stress amplitude sweep of preformed dECM hydrogel solutions at various concentration

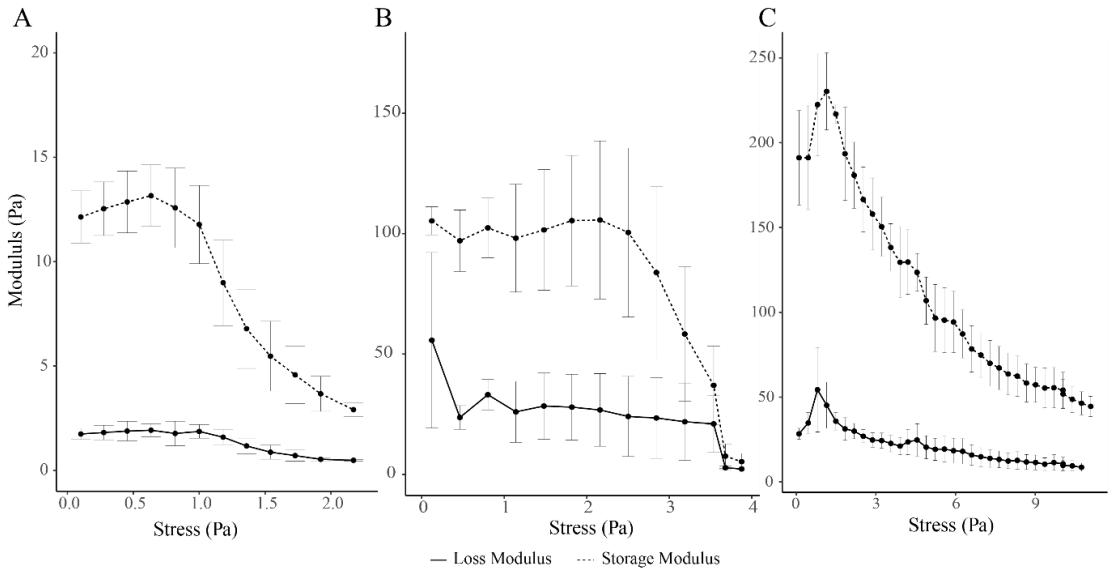

Note. Stress amplitude ranged from 0.1 to 50 Pa or until the hydrogel reached its yield point as indicated. Frequency and temperature remained constant (0.169 Hz at 37°C). (**A**) 3mg/ml dECM hydrogel, (**B**) 6mg/ml dECM hydrogel, (**C**) 8mg/ml dECM hydrogel. Data is represented as Mean ± SEM for n=3.

3.4 Degradation Test Results

3D degradation tests were used to investigate the stability of the hydrogels *in vitro*. The concentration of collagenase used (0.1 wt.%) is much higher than what would be seen in an *in vivo* environment and was specifically chosen to provide an accelerated assay to determine the rate of degradation [56]. Hydrogels were allowed 24 hours for full gelation and crosslinking prior to the degradation test. The degradation of the hydrogels was quantified as the % Mass remaining = the dry weight remaining of the control hydrogels exposed to PBS after 30-, 60-, 90- and 120-minutes relative to the hydrogels exposed to collagenase for the same amount of time. Collagenase at 0.1 wt% was utilized in order to

www.manaraa.com

determine the effects of genipin crosslinking at various concentrations on the rate of *in vitro* degradation of the dECM hydrogels. Crosslinking of the 8 mg/ml dECM hydrogels at all genipin concentrations provided considerable resistance to collagenase degradation in comparison to the 0 mM genipin hydrogels exposed to collagenase. Most notably, increased resistance to degradation was observed with increasing genipin concentration. Hydrogels crosslinked with 0.1, 0.5 or 1 mM genipin retained 50%, 80% and 81% of their mass by the end of the 120 min collagenase incubation (Figure 17). In comparison, control hydrogels containing no genipin which were exposed to collagenase were almost completed degraded at the end of the 120-minute time point (17.9% remaining). The 0.1mM genipin concentration slows degradation 4-fold based on masses obtained at 30 minutes vs 120 minutes. These results support the literature regarding the mechanism of action for collagenase degradation which occurs via the cleavage of amide bonds [108]. As previously mentioned, the mechanism behind genipin crosslinking is closely linked to nucleophilic attack on amine functional groups, therefore as genipin concentration with the dECM hydrogels increases, there is increased opposition to degradation due to the genipin strongly holding the collagen fragments together.

www.manaraa.com

Figure 12

3D degradation assay of genipin crosslinked dECM hydrogels

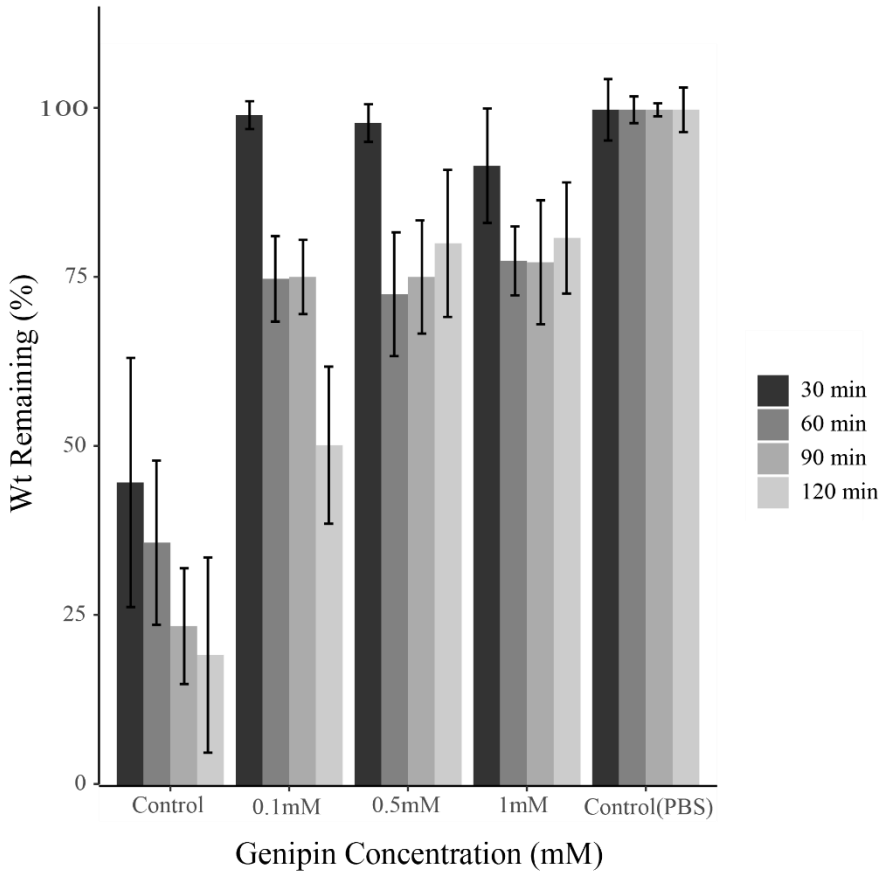

Note. Enzymatic degradation of dECM hydrogels at 30, 60, 90 and 120 minutes. Data is represented as the Mean ± SEM for n=3 at each time point and condition. Significance was identified between all groups (0, 0.1, 0.5, 1 mM) in comparison to the control hydrogels exposed to PBS.

3.5 In Vitro Biocompatibility Test Results

3.5.1 Live/Dead Assay

A Calcein-AM and Ethidium homodimer-1 (Invitrogen, Thermofisher) Live/Dead assay was utilized to qualitatively assess the cell viability of MSCs seeded on top of the

www.manaraa.com

hydrogels (2D), or within the bulk (3D). The Live/Dead assay consisted of Calcein-AM, a green-fluorescent stain which is present only in cells that are metabolically active within the field of view. If a cell stains green, it therefore qualifies as being alive. Alternatively, Ethidium homodimer-1, a red-fluorescent marker was included to specifically target membrane instability and loss of integrity. The loss of integrity and membrane instability indicates that the cells in the field of view are dying and/or dead. The number of live cells was quantified with a Nikon A-1 confocal scanning microscope and Fiji (ImageJ) as the average cell count of 5 different fields of view for hydrogels of each condition (control, 0.1 mM, 0.5 mM, and 1 mM genipin). 8 mg/ml hydrogels without genipin seeded with MSCs in 2D displayed a slight decrease in viability, however the viability was still >90% by day 7. Similarly, MSCs cultured within the bulk of control hydrogels also maintained consistently high viability over the course of seven days (>85%). MSCs cultured in 8 mg/ml dECM hydrogels at all genipin concentrations in 2D and 3D also displayed considerable viable by day 7. 1 mM genipin crosslinked hydrogels with cells seeded in 2D and 3D exhibited the lowest viability out of all genipin crosslinking concentrations by day 7 (65% viability in 2D and 63% viability in 3D)(Figure 18 and Figure 21). Viability was determined with confocal microscopy such that cells with green stained cytoplasm's without any simultaneous red nuclei staining were deemed viable. The 2D Live/Dead viability assay indicated no significance in the viability of cells seeded within the control hydrogels at days 1, 3 and 7, however there was significance established between the concentrations at day 7 and the respective control. There was no significance identified between concentrations and their respective controls at days 1 and 3, however significance was found between day 0.1, 0.5, and 1 mM genipin concentrations at day 7 in comparison

www.manaraa.com

to those same concentrations at day 1. Furthermore, there was no significance in cell viability observed between the concentration at day 3 and day 1. It is worth mentioning that this assay was not paired, and each time point did not utilize the same hydrogels for each concentration. Furthermore, there were inconsistencies in cell distribution which contributed to the overall variability of the data. As for 3D cell viability, the was no significance found between the controls at days 1, 3 and 7. Cell viability was found to be significant between hydrogels crosslinked with 0.5mM and 1mM genipin in comparison to the control at day 3. Furthermore, no significance was found between the concentrations at day 7 and the day 7 control. Additionally, no significance was established between any of the concentrations at day 3 and day 7 in comparison to their respective concentration day date 1.

8 mg/ml dECM hydrogels seeded in 2D and 3D without the addition of genipin exhibited high rates of cell growth and proliferation in comparison to the highest genipin concentration of 1 mM (Figure 19 and Figure 22). Throughout mostly all 2D Live/Dead staining and imaging, cell morphology was observed to be balled and rounded. This is consistent with previous findings that suggest MSCs seeded on top of soft matrices remained balled and exhibited limited spreading. This in direct comparison to seeding within the bulk on the hydrogel where soft matrices promote cell spreading and elongation [109, 110]. In a few instances, cells seeded in 3D hydrogels crosslinked with the lowest genipin concentration of 0.1 mM exhibited a unique trend between regarding MSC morphology. In comparison to the rounded morphology observed in the highest genipin concentrations, MSCs seeded in 3D hydrogels crosslinked with 0.1 mM genipin exhibited spreading and elongation (Figure A23 A,B,D and E). This suggests that when cells are

www.manaraa.com

seeded in a 3D matrix that is soft, spreading and elongation is promoted, however as the stiffness of the matrix increases, spreading is inhibited. Furthermore, similar effects on cell morphology and spreading have previously been demonstrated in research which involve genipin crosslinking of the hydrogel network [54, 111]. These findings indicate there may be a direct relationship between matrix stiffness, dimensionality and the spreading of MSCs, however additional studies should be conducted to further characterize the cytotoxic effects before potential *in vivo* studies can be performed.

www.manaraa.com

Figure 13

2D Cell Viability of MSC's seeded on genipin crosslinked hydrogels

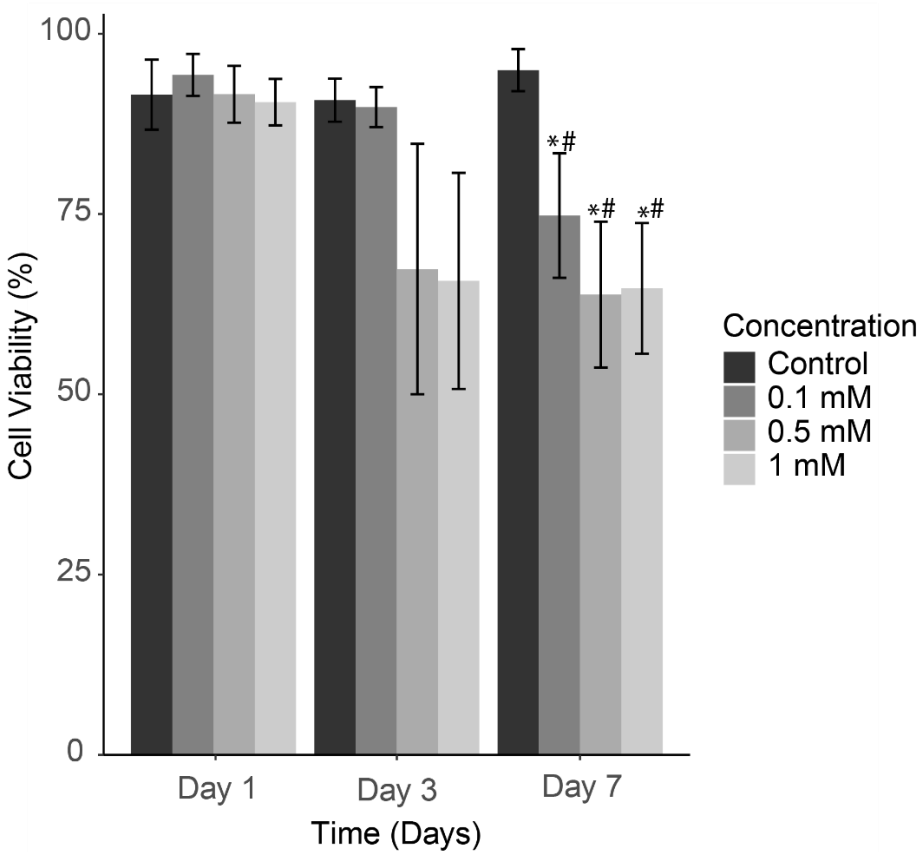

Note. Cell viability was assessed via a Live/Dead assay at days 1, 3 and 7 and the data is representative of Mean ± SEM for n=5 fields of view per condition with n=1 samples. *, significance between the concentration and control at day 7 ($p<0.05$). #, significant difference between the concentration at day 7 in comparison to the viability of that concentration at day 1 ($p<0.05$).

www.manaraa.com

Figure 14

Images of 2D Cell Viability of MSC's seeded on genipin crosslinked hydrogels

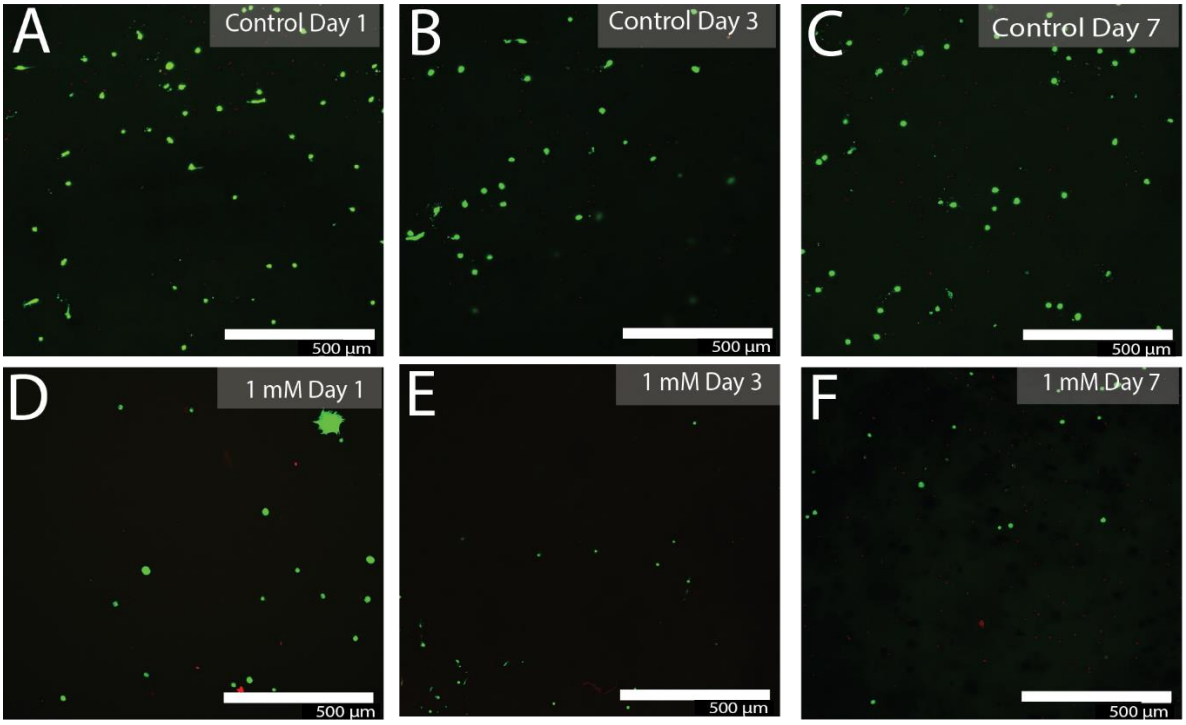

Note. Cell viability was assessed via a Live/Dead assay at days 1, 3 and 7 where Calcein AM stains green for live cells and Edth-1 stains red for dead cells . The full panel containing all genipin concentrations can be found in the Figure A6. Scale bars represent 500 µm for n=1 field of view.

www.manaraa.com

Figure 15

3D Cell Viability of MSC's seeded in the bulk of genipin crosslinked dECM hydrogels

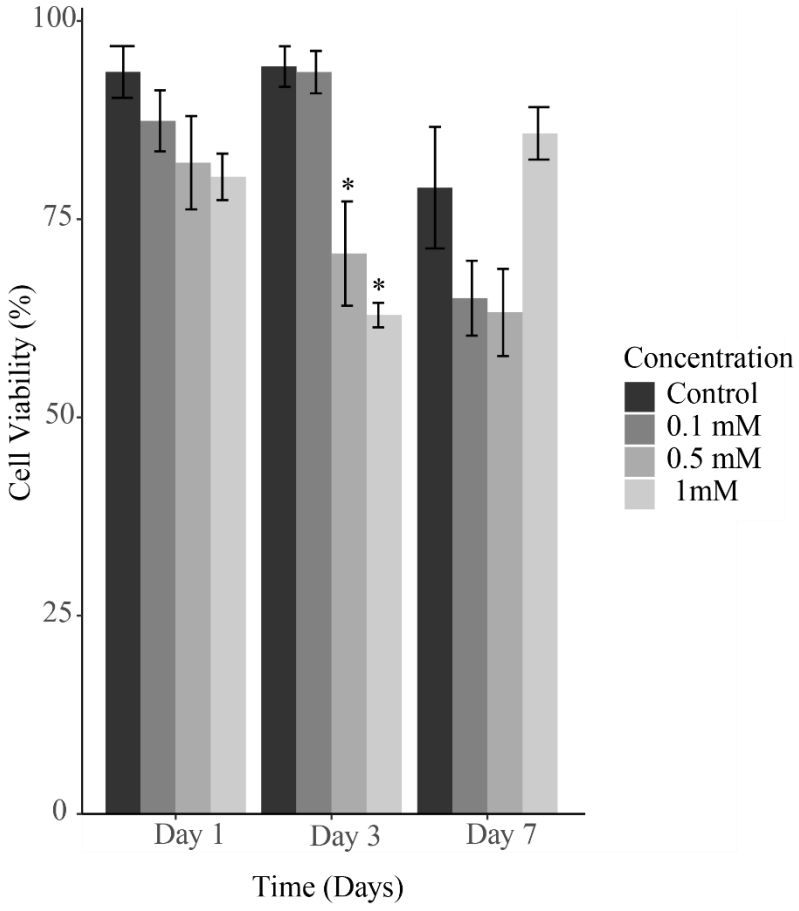

Note. Cell viability was assessed via a Live/Dead assay at days 1, 3 and 7 and the data is representative of Mean ± SEM for n=5 fields of view per condition. *, significance between the concentration and respective control at day 3 ($p<0.05$).

www.manaraa.com

Figure 16

Images of 3D Cell Viability of MSC's seeded on genipin crosslinked hydrogels

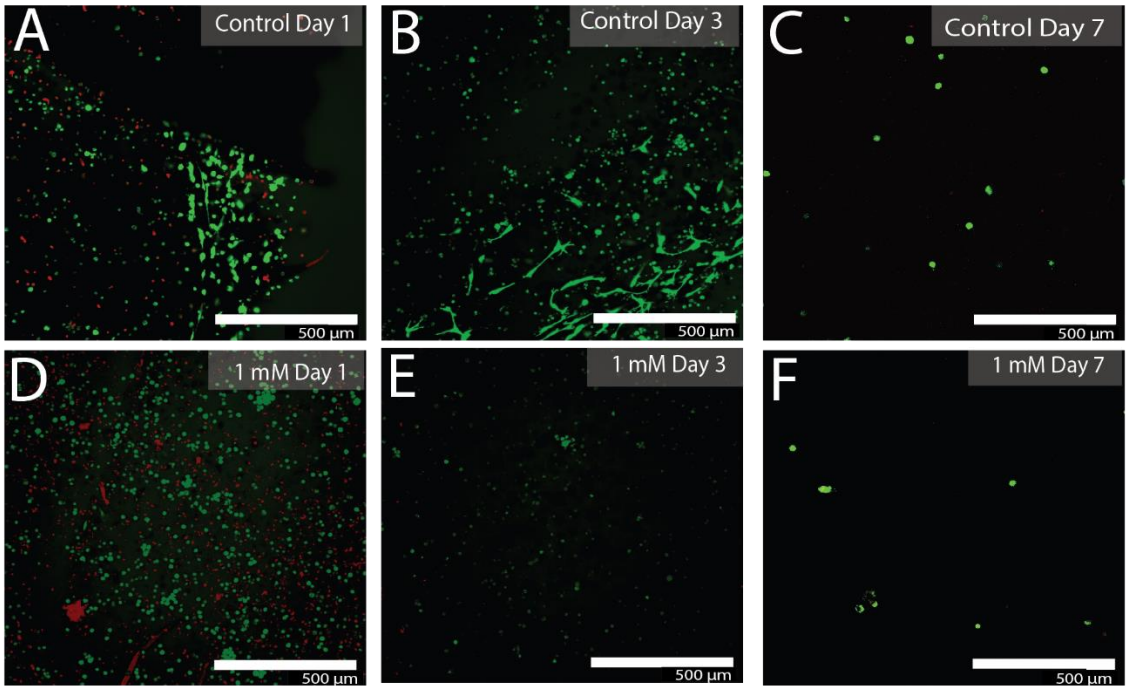

Note. Cell viability was assessed via a Live/Dead assay at days 1, 3 where Calcein AM stains green for live cells and Edth-1 stains red for dead cells. The full panel containing all genipin concentrations can be found in the Figure A7. Scale bars represent 500 µm for n=1.

3.5.2 Alamar Blue Assay

Alamar blue is a quantitative assay used to directly indicate cell viability. Cells exposed to alamar blue will undergo a colorimetric change depending on the amount of metabolic activity that the cell is capable of conducting. Therefore, the darker the color is observed, the less metabolic activity which indicates less viable cells. Results from the alamar blue assay conducted on 2D hydrogels indicate viability at all time points (1, 3 and 7 days) as indicated by high cells counts. Furthermore a clean trend was observed between the cell count and the concentration of genipin such that as genipin concentration increases,

www.manaraa.com

cell count decreases (Figure 24). This is in line with the previous findings from the Live/Dead assays conducted in 2D. It is worth nothing that the results obtained for 0.1 mM genipin crosslinked indicate negligible effects on cell viability due to the cell count being almost identical to the control.

An attempt to quantify cell counts from MSCs seeded in bulk of genipin crosslinked dECM hydrogels results were inconclusive and inconsistent. The standard utilized to quantify the number of cells in 3D was the same standard used for 2D quantification. However, numerous company websites suggest that standards created for 2D cultures are not comparable for 3D samples. This is due to differences in rates of adsorption between 2D and 3D systems. Additionally, it is possible that over the course of 7 days, excess genipin is leeching out of the hydrogels (because these gels were not washed prior to cell culture) which results in inconclusive readings.

www.manaraa.com

Figure 17

2D change in cell count determined by Alamar Blue

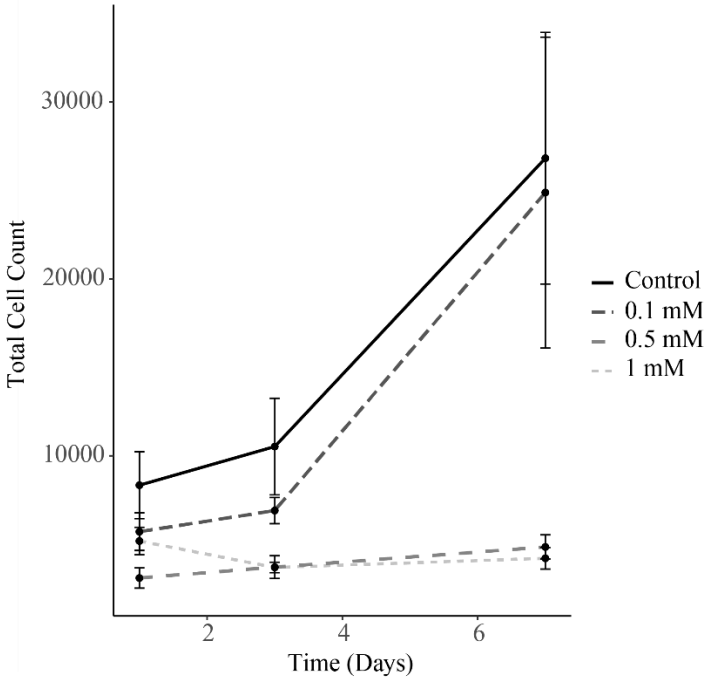

Note: Change in cell for MSCs seeded on the surface of dECM hydrogels crosslinked with genipin at 0.1, 0.5- and 1-mM concentrations. Data is representative of Mean ± SEM for n=4.

3.6 ECM Nanofiber Dip Coating Results

3.6.1 Nanofiber Fabrication

DiI-PCL nanofibers were fabricated utilizing an automated electrospinning set up (Figure A1). A rack was placed between the rotating parallel tracks to gather an overall evenly dense and distributed layer of DiI-PCL nanofibers. Alignment of PCL fibers was confirmed via brightfield imagining (Figure 25D and H) for both fibers dipped in 0 mM genipin dECM hydrogel solutions and 1 mM dECM hydrogel solutions.

www.manaraa.com

3.6.2 Cell Culture Results

DiI-stained PCL NF circular frames were dipped in either a dECM hydrogel solution containing MSCs with no genipin or a 1 mM genipin hydrogel solution. Following polymerization, the gel dip coated fibers containing embedded MSCs were assessed for cell viability using a Live/Dead stain at 1,3 and 7-days using confocal microscopy (Nikon). DiI staining of the PCL fibers was unable to be visualized at some time points, the reason is likely do to the dye being washed out or it may be that the Live/Dead Ethd-1 stain overpowered the DiI-stained fibers and therefore was unable to be captured via confocal microscopy.

PCL fibers dipped in the dECM hydrogel solution containing no genipin displayed a linear increase in viability over the course of the seven-day period. Specifically, day one viability was >75% , however by day 7 the viability had increased to 90% (Figure 26). The fluorescent cells in control hydrogels were visually observed at all time points and by day 7, mostly all of MSCs in an average of 3 fields of view had aligned and elongated in the direction of the aligned PCL nanofibers (Figure 25A-C). Aligned PCL fibers dipped in 1 mM genipin dECM hydrogel solution exhibited a mixed morphology on day 1 where some of the cells were observed to be aligning with the PCL nanofibers. However, other cells displayed a balled-up morphology, similar to the results obtained during Live/Dead analysis of dECM hydrogels crosslinked with 0.1, 0.5 and 1 mM genipin containing no nanofibers (Figure 24E-G). Cell viability of the MSCs seeded on the PCL dipped nanofibers was substantially different compared to the nanofibers dipped in a dECM solution containing no genipin. Day 1 viability of MSCs embedded in 1 mM dip coated hydrogels was 67% as opposed to 65% at day 3 and 28% on day 7 (Figure 25). For this

www.manaraa.com

experiment, no significance between 0 mM and 1 mM was observed in the PCL fibers dip coated in the control dECM hydrogel solution at days 1, 3 and 7. However, there was a significant difference is cell viability between the 1 mM dip coated fibers at day 7 in comparison to the 1 mM fibers at all other days as well as the fibers dipped in the control gel. The trend observed with the dip coated nanofiber is similar to that seen in hydrogels crosslinked with 1 mM genipin containing no fibers, such that at high concentrations genipin leads to a reduction in cell viability over time. Furthermore, this test demonstrated that the incorporation of highly aligned PCL NFs with the genipin crosslinked hydrogels does not restrict alignment. Therefore, it can be assumed that even at lower genipin concentrations, elongation and alignment will not be inhibited. However, this test was an n=1 therefore in order to fully comprehend the effects of genipin crosslinking on cell viability, orientation and morphology, more experiments must be conducted.

www.manaraa.com

Figure 18

Cell viability of dECM hydrogel dip coated aligned PCL nanofibers

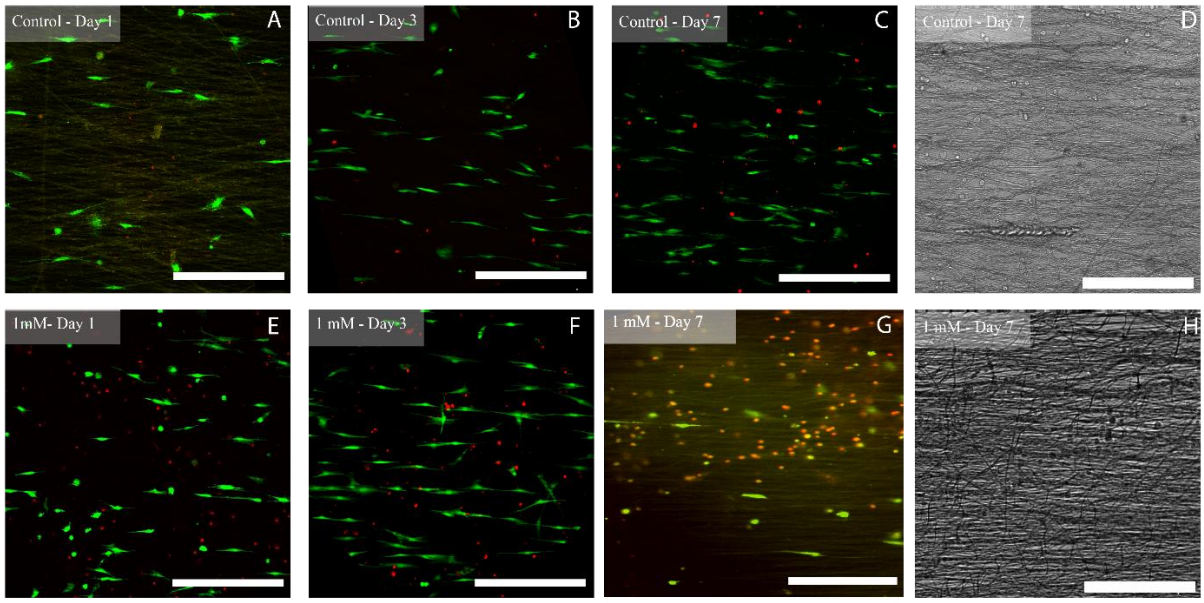

Note. A Live/Dead assay performed on control (A-D) and 1mM genipin(E-H) at days 1, 3 and 7. Calcein AM stains green for live cells and Edth-1 stains red for dead cells. Brightfield images (D and H) of control and 1mM at day 7 capture the orientation of PCL nanofibers found in all sample. Scale bars represent 500 μm for n=1.

www.manaraa.com

Figure 19

Cell viability of MSCs suspended in dECM hydrogel dip coated PCL nanofibers

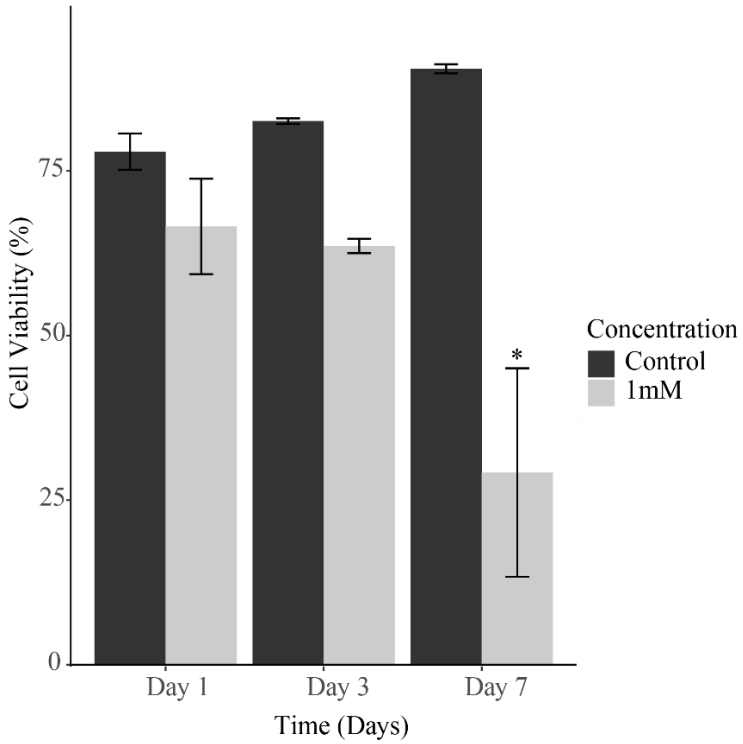

Note. The dECM hydrogel solutions investigated contained either no genipin or 1 mM genipin. Cell viability was assessed via a qualitative Live/Dead assay at days 1, 3 and 7. Data is representative of Mean ± SEM for n=1 with 3 fields of view. *, significance between the control and 1mM at 1, 3 and 7 ($p<0.001$)

www.manaraa.com

Chapter 4

Conclusions and Future Work

4.1 Conclusions

This research has been guided by the critical factors that should be taken into consideration when developing hydrogels for biomedical applications. The storage modulus of the hydrogel, which is indicative of stiffness, should be tunable such that the stiffness can be altered for a given applications. In addition, the hydrogel should induce little to no toxicity to cells that would be penetrating the hydrogel network. Furthermore, the hydrogel network should be biodegradable such that highly invasive, follow-up procedures and surgeries are not necessary.

Methods and techniques in this document were utilized to investigate the potential use of ECM hydrogels for translational biomedical applications. ECM hydrogels are utilized in biomedical applications due to their high biocompatibility and their ability to promote tissue repair regeneration. One of the biggest reasons that ECM hydrogels are an attractive option for regenerative medicine is that they contain proper ratios of biomolecules required for the complex bioactivity that occurs within natural tissue. However ECM hydrogels are often physically weak and have minimal structural stability. In addition, ECM hydrogels tend to have very quick in-vivo degradations. Therefore, the techniques utilized in this research were aimed at improving the limited structural stability and rapid degradation rates by introducing a chemical crosslinker, genipin. The genipin crosslinked hydrogels were evaluated in terms of their ability to improve the hydrogels mechanical properties and provide enhanced resistance to degradation. Furthermore, the

www.manaraa.com

genipin crosslinked gels were investigated to determine the morphological, organization and cytotoxic effects on cells seeded on the surface and within the bulk of the hydrogel.

The results presented in this research suggest that the methods and techniques utilized to decellularize the tendon and remove mostly all cellular content was successful. Furthermore, it has been demonstrated that bovine derived dECM can be solubilized and induced by changes in temperature and pH to form an elastic hydrogel structure. Through rheological characterization, numerous relationships were elucidated between the concentration of ECM and genipin, and their corresponding effects on the dECM hydrogels. As the concentration of both ECM and genipin increase, an increase in mechanical stiffness is observed. The crosslinking of dECM hydrogels leads to the formation of a strong elastic network that is more stable than that of pure, uncrosslinked dECM hydrogels. Similarly, the greater the concentration of genipin, the greater resistance to degradation the dECM hydrogels displayed. Distinct trends were also observed when investigating the effects of genipin crosslinking on MSC viability when seeded on the surface and in the bulk of dECM hydrogels. MSCs seeded in 2D and 3D genipin crosslinked hydrogels displayed slight effects on viability where the higher the genipin concentration, the more negative effect on MSC viability. In addition, the higher the genipin concentration, the more effects on MSC morphology was observed. Similar trends of MSC viability were also observed in dECM hydrogel dip coated aligned PCL nanofibers. Aligned PCL nanofibers also promoted MSC alignment and elongation in the direction of the nanofibers.

www.manaraa.com

4.2 Future Work

Although the data presented in this research is promising for the potential use of dECM hydrogels in translational applications, there are still a number of studies that must be conducted in order to completely comprehend this complex system. Further characterization of the hydrogel network should be conducted including SEM to determine the hydrogel microstructure and the effects of increasing dECM and genipin concentrations on the microstructure. Additionally, the degree of crosslinking within the hydrogels should be investigated where the degree of crosslinking is related to the percent of amine groups that have adhered to genipin molecules. Furthermore, the hydrogels swelling ratio, or the increase in weight due to absorption of fluids should be evaluated to determine if genipin crosslinking has a significant effect on the hydrogels ability to swell and resist dissolution.

Furthermore, although this research has demonstrated that the rate of degradation in dECM hydrogels can be tuned through the genipin concentration, the collagenase concentration utilized was much higher than what is typically found in the body. Therefore, studies should be conducted to determine how the *in vitro* results may translate in an *in vivo* setting. The effects of altered collagenase concentrations on dECM hydrogel degradation should also be evaluated. Based on the findings in this research, genipin crosslinked hydrogels displayed an increased resistance to degradation over the course of 2 hours may experience an even slower rate of degradation *in vivo* due to a lower concentration of collagenase being present.

Additional studies must be conducted to thoroughly investigate the effects of genipin crosslinking on cell interaction in 2D and 3D environments. Further cell studies must also be completed on aligned PCL nanofibers dip coated in dECM hydrogel solutions

www.manaraa.com

containing MSCs. In this research only dECM hydrogel solutions containing no genipin and 1 mM genipin were investigated for the sake of time. Also, only one fluorescent dye was utilized to visualize the nanofibers (DiI). Future studies should evaluate the viability of MSCs in various samples exposed to genipin concentrations between 0 mM and 1mM as well as investigate the use of a different fluorescent dye such as Hoechst blue to stain the aligned nanofibers. An additional study that may be interesting to conduct would be to assess MSC viability, morphology and orientation at a time point past 7 days to determine whether or not the cells would eventually spread when cultured in 2D and 3D environments.

The overarching goal of this research was to develop a naturally derived hydrogel consisting of dECM that can be incorporated with other biomaterials such as nanofibers. The hydrogels developed in this research demonstrated distinct structural, mechanical and biochemical properties. With the incorporation of nanofibers into a natural derived matrix, the goal was to direct cell alignment and guide tissue regeneration. This research has put forth the first steps towards completion of this goal by development of a naturally derived ECM hydrogel and identified unique properties that indicates the potential usability in translational applications. The successful completion of the goals outlined in this research is contingent upon the success of the future experiments that must be conducted as well as in depth *in vivo* analysis of this complex system.

www.manaraa.com

References

[1] M. A. Enas, "Hydrogel: Preparation, characterization, and applications: A review," *Journal of Advanced Research*, vol. 6, no. 2, pp. 105-121, 2015.

[2] O. Wichterle and D. LÍM, "Hydrophilic Gels for Biological Use," *Nature*, vol. 185, no. 4706, pp. 117-118, 1960/01/01 1960.

[3] Q. Chai, Y. Jiao, and X. Yu, "Hydrogels for Biomedical Applications: Their Characteristics and the Mechanisms behind Them," (in eng), *Gels (Basel, Switzerland)*, vol. 3, no. 1, p. 6, 2017.

[4] J. Tavakoli and Y. Tang, "Hydrogel Based Sensors for Biomedical Applications: An Updated Review," *Polymers*, vol. 9, no. 8, 2017.

[5] S. B. Mishra and A. K. Mishra, "Polymeric Hydrogels: A Review of Recent Developments," in *Polymeric Hydrogels as Smart Biomaterials*, S. Kalia, Ed. Cham: Springer International Publishing, 2016, pp. 1-17.

[6] U. S. K. Madduma-Bandarage and S. V. Madihally, "Synthetic hydrogels: Synthesis, novel trends, and applications," *Journal of Applied Polymer Science*, https://doi.org/10.1002/app.50376 vol. 138, no. 19, p. 50376, 2021/05/15 2021.

[7] S. Jiang, S. Liu, and W. Feng, "PVA hydrogel properties for biomedical application," *Journal of the Mechanical Behavior of Biomedical Materials*, vol. 4, no. 7, pp. 1228-1233, 2011/10/01/ 2011.

[8] C. C. Lin and K. S. Anseth, "PEG hydrogels for the controlled release of biomolecules in regenerative medicine," *Pharm Res*, vol. 26, no. 3, pp. 631-43, Mar 2009.

[9] M. F. Passos *et al.*, "pHEMA hydrogels," *Journal of Thermal Analysis and Calorimetry*, vol. 125, no. 1, pp. 361-368, 2016/07/01 2016.

[10] M. Zhu, Y. Wang, G. Ferracci, J. Zheng, N.-J. Cho, and B. H. Lee, "Gelatin methacryloyl and its hydrogels with an exceptional degree of controllability and batch-to-batch consistency," *Scientific Reports*, vol. 9, no. 1, p. 6863, 2019/05/03 2019.

[11] M. C. Catoira, L. Fusaro, D. Di Francesco, M. Ramella, and F. Boccafoschi, "Overview of natural hydrogels for regenerative medicine applications," *Journal of Materials Science: Materials in Medicine*, vol. 30, no. 10, p. 115, 2019/10/10 2019.

www.manaraa.com

[12] L. Cen, W. Liu, L. Cui, W. Zhang, and Y. Cao, "Collagen Tissue Engineering: Development of Novel Biomaterials and Applications," *Pediatric Research,* vol. 63, no. 5, pp. 492-496, 2008/05/01 2008.

[13] K. M. Pawelec, S. M. Best, and R. E. Cameron, "Collagen: a network for regenerative medicine," *J Mater Chem B,* vol. 4, no. 40, pp. 6484-6496, Oct 28 2016.

[14] M. Litwiniuk, A. Krejner, M. S. Speyrer, A. R. Gauto, and T. Grzela, "Hyaluronic Acid in Inflammation and Tissue Regeneration," *Wounds,* vol. 28, no. 3, pp. 78-88, Mar 2016.

[15] D. Jiang, J. Liang, and P. W. Noble, "Hyaluronan in tissue injury and repair," *Annu Rev Cell Dev Biol,* vol. 23, pp. 435-61, 2007.

[16] D. A. Gyles, L. D. Castro, J. O. C. Silva, and R. M. Ribeiro-Costa, "A review of the designs and prominent biomedical advances of natural and synthetic hydrogel formulations," *European Polymer Journal,* vol. 88, pp. 373-392, 2017/03/01/ 2017.

[17] A. M. Hawkins, "IODEGRADABLE HYDROGELS AND NANOCOMPOSITE POLYMERS: SYNTHESIS AND CHARACTERIZATION FOR BIOMEDICAL APPLICATIONS," 2012.

[18] P. M. Crapo, T. W. Gilbert, and S. F. Badylak, "An overview of tissue and whole organ decellularization processes," *Biomaterials,* vol. 32, no. 12, pp. 3233-43, Apr 2011.

[19] J. Kopecek, "Hydrogels: From soft contact lenses and implants to self-assembled nanomaterials," *Journal of Polymer Science Part A: Polymer Chemistry,* https://doi.org/10.1002/pola.23607 vol. 47, no. 22, pp. 5929-5946, 2009/11/15 2009.

[20] S.-H. Hyon, W.-I. Cha, Y. Ikada, M. Kita, Y. Ogura, and Y. Honda, "Poly(vinyl alcohol) hydrogels as soft contact lens material," *Journal of Biomaterials Science, Polymer Edition,* vol. 5, no. 5, pp. 397-406, 1994/01/01 1994.

[21] E. M. Ahmed, "Hydrogel: Preparation, characterization, and applications: A review," *Journal of Advanced Research,* vol. 6, no. 2, pp. 105-121, 2015/03/01/ 2015.

[22] J. W. Freeman *et al.*, "Evaluation of a hydrogel-fiber composite for ACL tissue engineering," *J Biomech,* vol. 44, no. 4, pp. 694-9, Feb 24 2011.

[23] J. Zhu and R. E. Marchant, "Design properties of hydrogel tissue-engineering scaffolds," *Expert Rev Med Devices,* vol. 8, no. 5, pp. 607-26, Sep 2011.

www.manaraa.com

[24] S. Kubinova, "Extracellular matrix based biomaterials for central nervous system tissue repair: the benefits and drawbacks," *Neural Regeneration Research,* vol. 12, no. 9, pp. 1430-1432, 2017.

[25] B. Ma, X. Wang, C. Wu, and J. Chang, "Crosslinking strategies for preparation of extracellular matrix-derived cardiovascular scaffolds," *Regen Biomater,* vol. 1, no. 1, pp. 81-9, Nov 2014.

[26] L. Voorhaar and R. Hoogenboom, "Supramolecular polymer networks: hydrogels and bulk materials," *Chemical Society Reviews,* 10.1039/C6CS00130K vol. 45, no. 14, pp. 4013-4031, 2016.

[27] W. Hu, Z. Wang, Y. Xiao, S. Zhang, and J. Wang, "Advances in crosslinking strategies of biomedical hydrogels," *Biomater Sci,* vol. 7, no. 3, pp. 843-855, Feb 26 2019.

[28] W. E. Hennink and C. F. van Nostrum, "Novel crosslinking methods to design hydrogels," *Advanced Drug Delivery Reviews,* vol. 64, pp. 223-236, 2012/12/01/ 2012.

[29] C. Hassan and N. Peppas, "Structure and Morphology of Freeze/Thawed PVA Hydrogels," *Macromolecules,* vol. 33, 03/11 2000.

[30] M. D. Au - Figueroa-Pizano, I. Au - Vélaz, and M. E. Au - Martínez-Barbosa, "A Freeze-Thawing Method to Prepare Chitosan-Poly(vinyl alcohol) Hydrogels Without Crosslinking Agents and Diflunisal Release Studies," *JoVE,* no. 155, p. e59636, 2020/01/14/ 2020.

[31] M. J. Moura, H. Faneca, M. P. Lima, M. H. Gil, and M. M. Figueiredo, "In situ forming chitosan hydrogels prepared via ionic/covalent co-cross-linking," *Biomacromolecules,* vol. 12, no. 9, pp. 3275-84, Sep 12 2011.

[32] A. Chenite *et al.*, "Novel injectable neutral solutions of chitosan form biodegradable gels in situ," *Biomaterials,* vol. 21, no. 21, pp. 2155-2161, 2000/11/01/ 2000.

[33] V. L. Deringer, U. Englert, and R. Dronskowski, "Covalency of hydrogen bonds in solids revisited," *Chem Commun (Camb),* vol. 50, no. 78, pp. 11547-9, Oct 9 2014.

[34] X. Dai *et al.*, "A Mechanically Strong, Highly Stable, Thermoplastic, and Self-Healable Supramolecular Polymer Hydrogel," *Advanced Materials,* https://doi.org/10.1002/adma.201500534 vol. 27, no. 23, pp. 3566-3571, 2015/06/01 2015.

www.manaraa.com

[35] S. Förster and M. Antonietti, "Amphiphilic Block Copolymers in Structure-Controlled Nanomaterial Hybrids," *Advanced Materials*, https://doi.org/10.1002/(SICI)1521-4095(199802)10:3<195::AID-ADMA195>3.0.CO;2-V vol. 10, no. 3, pp. 195-217, 1998/02/01 1998.

[36] M. Boffito, P. Sirianni, A. M. Di Rienzo, and V. Chiono, "Thermosensitive block copolymer hydrogels based on poly(varepsilon-caprolactone) and polyethylene glycol for biomedical applications: state of the art and future perspectives," *J Biomed Mater Res A*, vol. 103, no. 3, pp. 1276-90, Mar 2015.

[37] C. Martin, N. Aibani, J. F. Callan, and B. Callan, "Recent advances in amphiphilic polymers for simultaneous delivery of hydrophobic and hydrophilic drugs," *Ther Deliv*, vol. 7, no. 1, pp. 15-31, 2016.

[38] K. T. Nguyen and J. L. West, "Photopolymerizable hydrogels for tissue engineering applications," *Biomaterials*, vol. 23, no. 22, pp. 4307-14, Nov 2002.

[39] Y. D. Park, N. Tirelli, and J. A. Hubbell, "Photopolymerized hyaluronic acid-based hydrogels and interpenetrating networks," *Biomaterials*, vol. 24, no. 6, pp. 893-900, Mar 2003.

[40] H. Lin *et al.*, "Application of visible light-based projection stereolithography for live cell-scaffold fabrication with designed architecture," *Biomaterials*, vol. 34, no. 2, pp. 331-9, Jan 2013.

[41] G. M. Fernandes-Cunha, H. J. Lee, A. Kumar, A. Kreymerman, S. Heilshorn, and D. Myung, "Immobilization of Growth Factors to Collagen Surfaces Using Pulsed Visible Light," *Biomacromolecules*, vol. 18, no. 10, pp. 3185-3196, Oct 9 2017.

[42] R. P. Sinha and D. P. Hader, "UV-induced DNA damage and repair: a review," *Photochem Photobiol Sci*, vol. 1, no. 4, pp. 225-36, Apr 2002.

[43] L. S. Teixeira, J. Feijen, C. A. van Blitterswijk, P. J. Dijkstra, and M. Karperien, "Enzyme-catalyzed crosslinkable hydrogels: emerging strategies for tissue engineering," *Biomaterials*, vol. 33, no. 5, pp. 1281-90, Feb 2012.

[44] A. Abu-Hakmeh *et al.*, "Sequential gelation of tyramine-substituted hyaluronic acid hydrogels enhances mechanical integrity and cell viability," *Medical & Biological Engineering & Computing*, vol. 54, no. 12, pp. 1893-1902, 2016/12/01 2016.

[45] J. J. Sperinde and L. G. Griffith, "Control and Prediction of Gelation Kinetics in Enzymatically Cross-Linked Poly(ethylene glycol) Hydrogels," *Macromolecules*, vol. 33, no. 15, pp. 5476-5480, 2000/07/01 2000.

www.manaraa.com

[46] W. S. Dai and T. A. Barbari, "Hydrogel membranes with mesh size asymmetry based on the gradient crosslinking of poly(vinyl alcohol)," *Journal of Membrane Science,* vol. 156, no. 1, pp. 67-79, 1999/04/24/ 1999.

[47] J. E. Gough, C. A. Scotchford, and S. Downes, "Cytotoxicity of glutaraldehyde crosslinked collagen/poly(vinyl alcohol) films is by the mechanism of apoptosis," *J Biomed Mater Res,* vol. 61, no. 1, pp. 121-30, Jul 2002.

[48] B. D. Mather, K. Viswanathan, K. M. Miller, and T. E. Long, "Michael addition reactions in macromolecular design for emerging technologies," *Progress in Polymer Science,* vol. 31, no. 5, pp. 487-531, 2006/05/01/ 2006.

[49] R. D. Little, M. R. Masjedizadeh, O. Wallquist, and J. I. McLoughlin, "The Intramolecular Michael Reaction," *Organic Reactions,* https://doi.org/10.1002/0471264180.or047.02 pp. 315-552, 2004/10/15 2004.

[50] C. Echalier, L. Valot, J. Martinez, A. Mehdi, and G. Subra, "Chemical cross-linking methods for cell encapsulation in hydrogels," *Materials Today Communications,* vol. 20, p. 100536, 2019/09/01/ 2019.

[51] X. Sui, L. van Ingen, M. A. Hempenius, and G. J. Vancso, "Preparation of a Rapidly Forming Poly(ferrocenylsilane)-Poly(ethylene glycol)-based Hydrogel by a Thiol-Michael Addition Click Reaction," *Macromolecular Rapid Communications,* https://doi.org/10.1002/marc.201000420 vol. 31, no. 23, pp. 2059-2063, 2010/12/01 2010.

[52] J. S. Yoo, Y. J. Kim, S. H. Kim, and S. H. Choi, "Study on genipin: a new alternative natural crosslinking agent for fixing heterograft tissue," *Korean J Thorac Cardiovasc Surg,* vol. 44, no. 3, pp. 197-207, Jun 2011.

[53] S.-M. Lien, W.-T. Li, and T.-J. Huang, "Genipin-crosslinked gelatin scaffolds for articular cartilage tissue engineering with a novel crosslinking method," *Materials Science and Engineering: C,* vol. 28, no. 1, pp. 36-43, 2008/01/10/ 2008.

[54] R. M. Schek, A. J. Michalek, and J. C. Iatridis, "Genipin-crosslinked fibrin hydrogels as a potential adhesive to augment intervertebral disc annulus repair," *Eur Cell Mater,* vol. 21, pp. 373-83, Apr 18 2011.

[55] R. A. A. Muzzarelli, "Genipin-crosslinked chitosan hydrogels as biomedical and pharmaceutical aids," *Carbohydrate Polymers,* vol. 77, no. 1, pp. 1-9, 2009/05/22/ 2009.

[56] K. Výborný *et al.,* "Genipin and EDC crosslinking of extracellular matrix hydrogel derived from human umbilical cord for neural tissue repair," *Scientific Reports,* vol. 9, no. 1, p. 10674, 2019/07/23 2019.

www.manaraa.com

[57] R. Touyama *et al.*, "Studies on the Blue Pigments Produced from Genipin and Methylamine. II .On the Formation Mechanisms of Brownish-Red Intermediates Leading to the Blue Pigment Formation," *CHEMICAL & PHARMACEUTICAL BULLETIN*, vol. 42, no. 8, pp. 1571-1578, 1994.

[58] M. F. Butler, Y.-F. Ng, and P. D. A. Pudney, "Mechanism and kinetics of the crosslinking reaction between biopolymers containing primary amine groups and genipin," *Journal of Polymer Science Part A: Polymer Chemistry*, https://doi.org/10.1002/pola.10960 vol. 41, no. 24, pp. 3941-3953, 2003/12/15 2003.

[59] R. Touyama *et al.*, "Studies on the Blue Pigments Produced from Genipin and Methylamine. I. Structures of the Brownish-Red Pigments, Intermediates Leading to the Blue Pigments," *CHEMICAL & PHARMACEUTICAL BULLETIN*, vol. 42, no. 3, pp. 668-673, 1994.

[60] J. Jin, M. Song, and D. J. Hourston, "Novel Chitosan-Based Films Cross-Linked by Genipin with Improved Physical Properties," *Biomacromolecules*, vol. 5, no. 1, pp. 162-168, 2004/01/01 2004.

[61] H. W. Sung, R. N. Huang, L. L. Huang, and C. C. Tsai, "In vitro evaluation of cytotoxicity of a naturally occurring cross-linking reagent for biological tissue fixation," *J Biomater Sci Polym Ed*, vol. 10, no. 1, pp. 63-78, 1999.

[62] H. J. Koo, K. H. Lim, H. J. Jung, and E. H. Park, "Anti-inflammatory evaluation of gardenia extract, geniposide and genipin," *J Ethnopharmacol*, vol. 103, no. 3, pp. 496-500, Feb 20 2006.

[63] A. G. MacDiarmid *et al.*, "Electrostatically-generated nanofibers of electronic polymers," *Synthetic Metals*, vol. 119, no. 1, pp. 27-30, 2001/03/15/ 2001.

[64] C.-C. Yu *et al.*, "Random and aligned electrospun PLGA nanofibers embedded in microfluidic chips for cancer cell isolation and integration with air foam technology for cell release," *Journal of Nanobiotechnology*, vol. 17, no. 1, p. 31, 2019/02/19 2019.

[65] F. Yang, R. Murugan, S. Wang, and S. Ramakrishna, "Electrospinning of nano/micro scale poly(L-lactic acid) aligned fibers and their potential in neural tissue engineering," *Biomaterials*, vol. 26, no. 15, pp. 2603-10, May 2005.

[66] V. Chaurey *et al.*, "Nanofiber size-dependent sensitivity of fibroblast directionality to the methodology for scaffold alignment," *Acta Biomater*, vol. 8, no. 11, pp. 3982-90, Nov 2012.

www.manaraa.com

[67] Z. Zhao *et al.*, "[Influence of aligned electrospinning poly (propylene carbonate) on axonal growth of dorsal root ganglion in vitro]," *Zhongguo Xiu Fu Chong Jian Wai Ke Za Zhi*, vol. 25, no. 2, pp. 171-5, Feb 2011.

[68] W.-J. Li, R. M. Shanti, and R. S. Tuan, "Electrospinning Technology for Nanofibrous Scaffolds in Tissue Engineering," *Nanotechnologies for the Life Sciences*, https://doi.org/10.1002/9783527610419.ntls0097 2007/09/15 2007.

[69] T. Subbiah, G. S. Bhat, R. W. Tock, S. Parameswaran, and S. S. Ramkumar, "Electrospinning of nanofibers," *Journal of Applied Polymer Science*, https://doi.org/10.1002/app.21481 vol. 96, no. 2, pp. 557-569, 2005/04/15 2005.

[70] D. H. Reneker and I. Chun, "Nanometre diameter fibres of polymer, produced by electrospinning," *Nanotechnology*, vol. 7, no. 3, pp. 216-223, 1996/09/01 1996.

[71] G. I. Taylor and M. D. Van Dyke, "Electrically driven jets," *Proceedings of the Royal Society of London. A. Mathematical and Physical Sciences*, vol. 313, no. 1515, pp. 453-475, 1969/12/02 1969.

[72] J. Xue, T. Wu, Y. Dai, and Y. Xia, "Electrospinning and Electrospun Nanofibers: Methods, Materials, and Applications," *Chem Rev*, vol. 119, no. 8, pp. 5298-5415, Apr 24 2019.

[73] C. M. Vaz, S. van Tuijl, C. V. C. Bouten, and F. P. T. Baaijens, "Design of scaffolds for blood vessel tissue engineering using a multi-layering electrospinning technique," *Acta Biomaterialia*, vol. 1, no. 5, pp. 575-582, 2005/09/01/ 2005.

[74] Z.-M. Huang, Y. Z. Zhang, M. Kotaki, and S. Ramakrishna, "A review on polymer nanofibers by electrospinning and their applications in nanocomposites," *Composites Science and Technology*, vol. 63, no. 15, pp. 2223-2253, 2003/11/01/ 2003.

[75] V. Beachley, E. Katsanevakis, N. Zhang, and X. Wen, "A novel method to precisely assemble loose nanofiber structures for regenerative medicine applications," *Adv Healthc Mater*, vol. 2, no. 2, pp. 343-51, Feb 2013.

[76] I. Alghoraibi and S. Alomari, "Different Methods for Nanofiber Design and Fabrication," in *Handbook of Nanofibers*, A. Barhoum, M. Bechelany, and A. Makhlouf, Eds. Cham: Springer International Publishing, 2018, pp. 1-46.

[77] H. E. Jeong, S. H. Lee, P. Kim, and K. Y. Suh, "Stretched polymer nanohairs by nanodrawing," *Nano Lett*, vol. 6, no. 7, pp. 1508-13, Jul 2006.

www.manaraa.com

[78] A. S. Nain, J. C. Wong, C. Amon, and M. Sitti, "Drawing suspended polymer micro-/nanofibers using glass micropipettes," *Applied Physics Letters,* vol. 89, no. 18, p. 183105, 2006/10/30 2006.

[79] D. Jao and V. Z. Beachley, "Continuous Dual-Track Fabrication of Polymer Micro-/Nanofibers Based on Direct Drawing," *ACS Macro Letters,* vol. 8, no. 5, pp. 588-595, 2019/05/21 2019.

[80] S. Grimm *et al.*, "Nondestructive Replication of Self-Ordered Nanoporous Alumina Membranes via Cross-Linked Polyacrylate Nanofiber Arrays," *Nano Letters,* vol. 8, no. 7, pp. 1954-1959, 2008/07/01 2008.

[81] H. Li, Y. Ke, and Y. Hu, "Polymer nanofibers prepared by template melt extrusion," *Journal of Applied Polymer Science,* https://doi.org/10.1002/app.22597 vol. 99, no. 3, pp. 1018-1023, 2006/02/05 2006.

[82] V. Beachley and X. Wen, "Polymer nanofibrous structures: Fabrication, biofunctionalization, and cell interactions," *Progress in Polymer Science,* vol. 35, no. 7, pp. 868-892, 2010/07/01/ 2010.

[83] J. D. Hartgerink, E. Beniash, and S. I. Stupp, "Self-assembly and mineralization of peptide-amphiphile nanofibers," *Science,* vol. 294, no. 5547, pp. 1684-8, Nov 23 2001.

[84] S. Zhang, "Fabrication of novel biomaterials through molecular self-assembly," *Nat Biotechnol,* vol. 21, no. 10, pp. 1171-8, Oct 2003.

[85] Y. Zhang, H. Ouyang, C. T. Lim, S. Ramakrishna, and Z. M. Huang, "Electrospinning of gelatin fibers and gelatin/PCL composite fibrous scaffolds," *J Biomed Mater Res B Appl Biomater,* vol. 72, no. 1, pp. 156-65, Jan 15 2005.

[86] A. Andrady, "Book Review of Science and Technology of Polymer Nanofibers," *Journal of the American Chemical Society,* vol. 130, no. 50, pp. 17204-17204, 2008/12/17 2008.

[87] Q. P. Pham, U. Sharma, and A. G. Mikos, "Electrospun Poly(ε-caprolactone) Microfiber and Multilayer Nanofiber/Microfiber Scaffolds: Characterization of Scaffolds and Measurement of Cellular Infiltration," *Biomacromolecules,* vol. 7, no. 10, pp. 2796-2805, 2006/10/01 2006.

[88] R. Kenawy el *et al.*, "Release of tetracycline hydrochloride from electrospun poly(ethylene-co-vinylacetate), poly(lactic acid), and a blend," *J Control Release,* vol. 81, no. 1-2, pp. 57-64, May 17 2002.

www.manaraa.com

[89] K. Kim *et al.*, "Control of degradation rate and hydrophilicity in electrospun non-woven poly(D,L-lactide) nanofiber scaffolds for biomedical applications," *Biomaterials,* vol. 24, no. 27, pp. 4977-85, Dec 2003.

[90] A. Chinnappan, C. Baskar, S. Baskar, G. Ratheesh, and S. Ramakrishna, "An overview of electrospun nanofibers and their application in energy storage, sensors and wearable/flexible electronics," *Journal of Materials Chemistry C,* 10.1039/C7TC03058D vol. 5, no. 48, pp. 12657-12673, 2017.

[91] S. Reich *et al.*, "Polymer nanofibre composite nonwovens with metal-like electrical conductivity," *npj Flexible Electronics,* vol. 2, no. 1, p. 5, 2018/02/14 2018.

[92] Z. Ma, M. Kotaki, R. Inai, and S. Ramakrishna, "Potential of nanofiber matrix as tissue-engineering scaffolds," *Tissue Eng,* vol. 11, no. 1-2, pp. 101-9, Jan-Feb 2005.

[93] J. Doshi and D. H. Reneker, "Electrospinning process and applications of electrospun fibers," *Journal of Electrostatics,* vol. 35, no. 2, pp. 151-160, 1995/08/01/ 1995.

[94] L. A. Smith and P. X. Ma, "Nano-fibrous scaffolds for tissue engineering," *Colloids Surf B Biointerfaces,* vol. 39, no. 3, pp. 125-31, Dec 10 2004.

[95] A. D. Schoenenberger, J. Foolen, P. Moor, U. Silvan, and J. G. Snedeker, "Substrate fiber alignment mediates tendon cell response to inflammatory signaling," *Acta Biomaterialia,* vol. 71, pp. 306-317, 2018/04/15/ 2018.

[96] M. J. Sawkins *et al.*, "Hydrogels derived from demineralized and decellularized bone extracellular matrix," *Acta Biomater,* vol. 9, no. 8, pp. 7865-73, Aug 2013.

[97] M. T. Wolf *et al.*, "A hydrogel derived from decellularized dermal extracellular matrix," *Biomaterials,* vol. 33, no. 29, pp. 7028-38, Oct 2012.

[98] A. Viswanath *et al.*, "Extracellular matrix-derived hydrogels for dental stem cell delivery," *J Biomed Mater Res A,* vol. 105, no. 1, pp. 319-328, Jan 2017.

[99] H. A. Barnes, J. F. Hutton, and K. Walters, *An introduction to rheology*. Elsevier, 1989.

[100] J. M. Zuidema, C. J. Rivet, R. J. Gilbert, and F. A. Morrison, "A protocol for rheological characterization of hydrogels for tissue engineering strategies," *Journal of Biomedical Materials Research Part B: Applied Biomaterials,* https://doi.org/10.1002/jbm.b.33088 vol. 102, no. 5, pp. 1063-1073, 2014/07/01 2014.

www.manaraa.com

[101] M. J. Moura, M. M. Figueiredo, and M. H. Gil, "Rheological Study of Genipin Cross-Linked Chitosan Hydrogels," *Biomacromolecules,* vol. 8, no. 12, pp. 3823-3829, 2007/12/01 2007.

[102] R. B. Bird, G. C. Dai, and B. J. Yarusso, "The Rheology and Flow of Viscoplastic Materials," *Reviews in Chemical Engineering,* vol. 1, no. 1, pp. 1-70, 1983.

[103] P. Coussot, L. Tocquer, C. Lanos, and G. Ovarlez, "Macroscopic vs. local rheology of yield stress fluids," *Journal of Non-Newtonian Fluid Mechanics,* vol. 158, no. 1, pp. 85-90, 2009/05/01/ 2009.

[104] V. Beachley and X. Wen, "Creating waved and aligned nanofiber composites to mimic the microstructure and match the compliance of blood vessels," in *8th World Biomaterials Congress 2008, WBC 2008*, 2008.

[105] A. A. Conte, K. Sun, X. Hu, and V. Z. Beachley, "Effects of Fiber Density and Strain Rate on the Mechanical Properties of Electrospun Polycaprolactone Nanofiber Mats," *Front Chem,* vol. 8, p. 610, 2020.

[106] S. Nagata, R. Hanayama, and K. Kawane, "Autoimmunity and the Clearance of Dead Cells," *Cell,* vol. 140, no. 5, pp. 619-630, 2010/03/05/ 2010.

[107] A. Franck, "Viscoelasticity and dynamic mechanical testing," p. 7.

[108] M. D. Shoulders and R. T. Raines, "Collagen structure and stability," *Annu Rev Biochem,* vol. 78, pp. 929-58, 2009.

[109] S. R. Caliari, S. L. Vega, M. Kwon, E. M. Soulas, and J. A. Burdick, "Dimensionality and spreading influence MSC YAP/TAZ signaling in hydrogel environments," *Biomaterials,* vol. 103, pp. 314-323, 2016/10/01/ 2016.

[110] L. G. Vincent, Y. S. Choi, B. Alonso-Latorre, J. C. del Alamo, and A. J. Engler, "Mesenchymal stem cell durotaxis depends on substrate stiffness gradient strength," *Biotechnol J,* vol. 8, no. 4, pp. 472-84, Apr 2013.

[111] D. J. Macaya, K. Hayakawa, K. Arai, and M. Spector, "Astrocyte infiltration into injectable collagen-based hydrogels containing FGF-2 to treat spinal cord injury," *Biomaterials,* vol. 34, no. 14, pp. 3591-602, May 2013.

www.manaraa.com

Appendix

Supplemental Data

Figure A1

The overall set-up for preparing electrospun PCL nanofibers with automated parallel tracks and the collecting rack below [105]

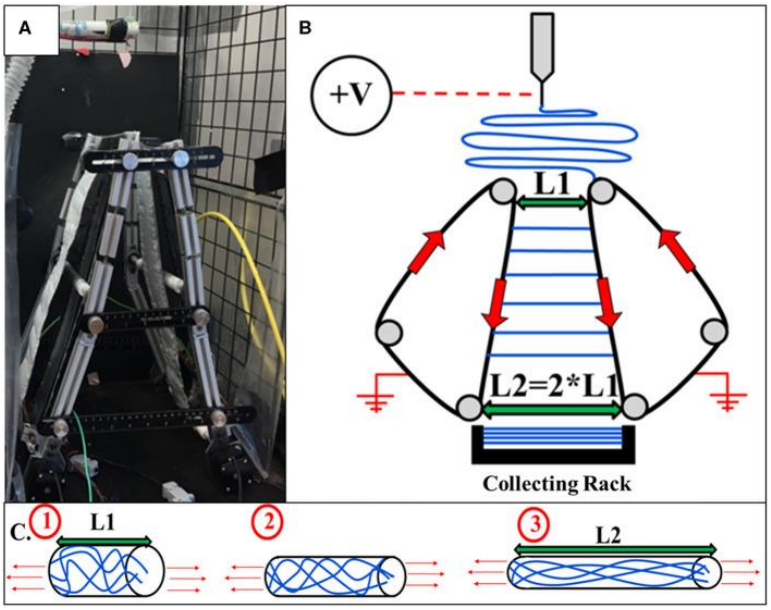

Figure A2

Genipin crosslinked 8 mg/ml dECM hydrogels prepared in a 24-well plate

Note. Genipin concentration from left to right: control (no genipin), 0.1mM, 0.5mM, 1mM Genipin

www.manaraa.com

Figure A3

Gelation Kinetics of 3mg/ml dECM hydrogel

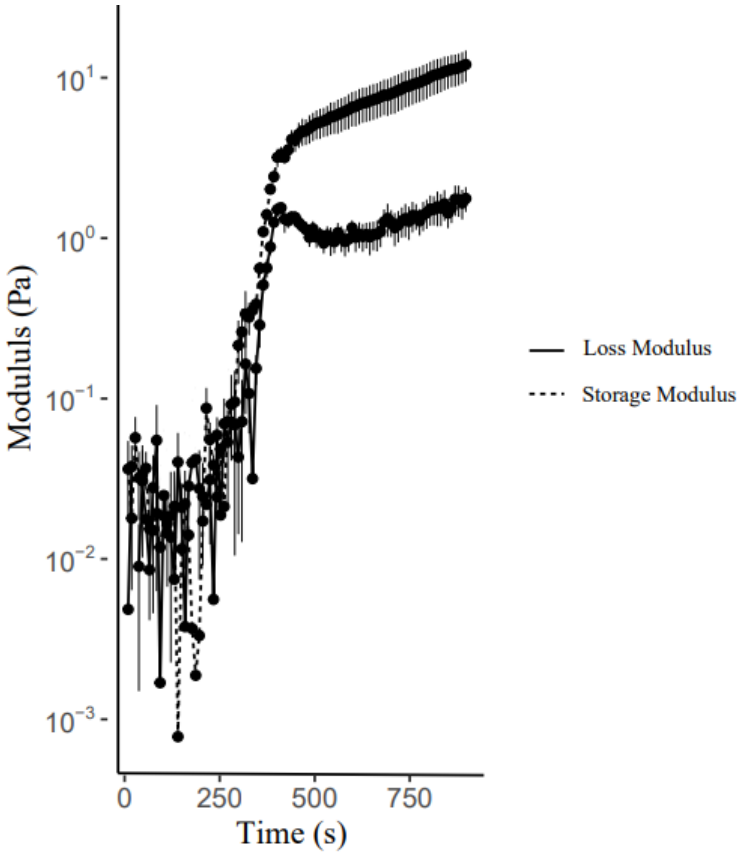

Note. Assessed by rheology with corresponding G' (Storage Modulus) and G"(Loss Modulus). Data is representative of n=3.

www.manaraa.com

Figure A4

Gelation Kinetics of 6mg/ml dECM hydrogel

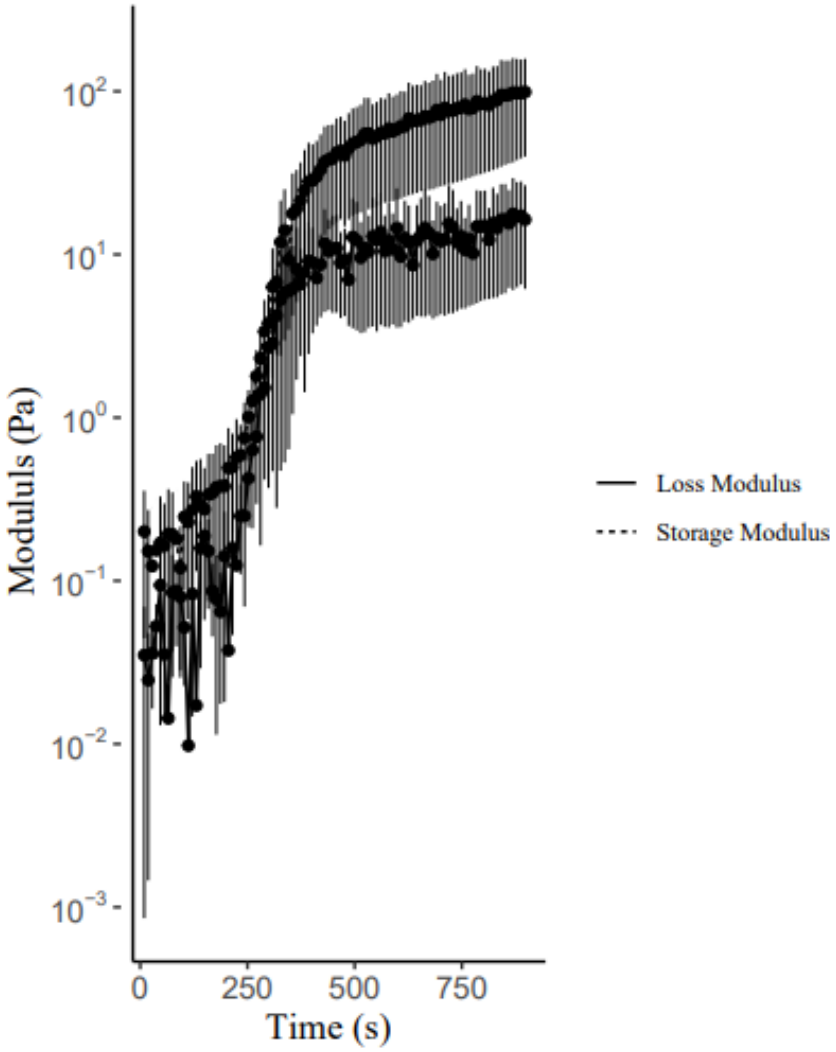

Note. Assessed by rheology with corresponding G' (Storage Modulus) and G"(Loss Modulus). Data is representative of n=3.

www.manaraa.com

Figure A5

Gelation Kinetics of 8mg/ml dECM hydrogel

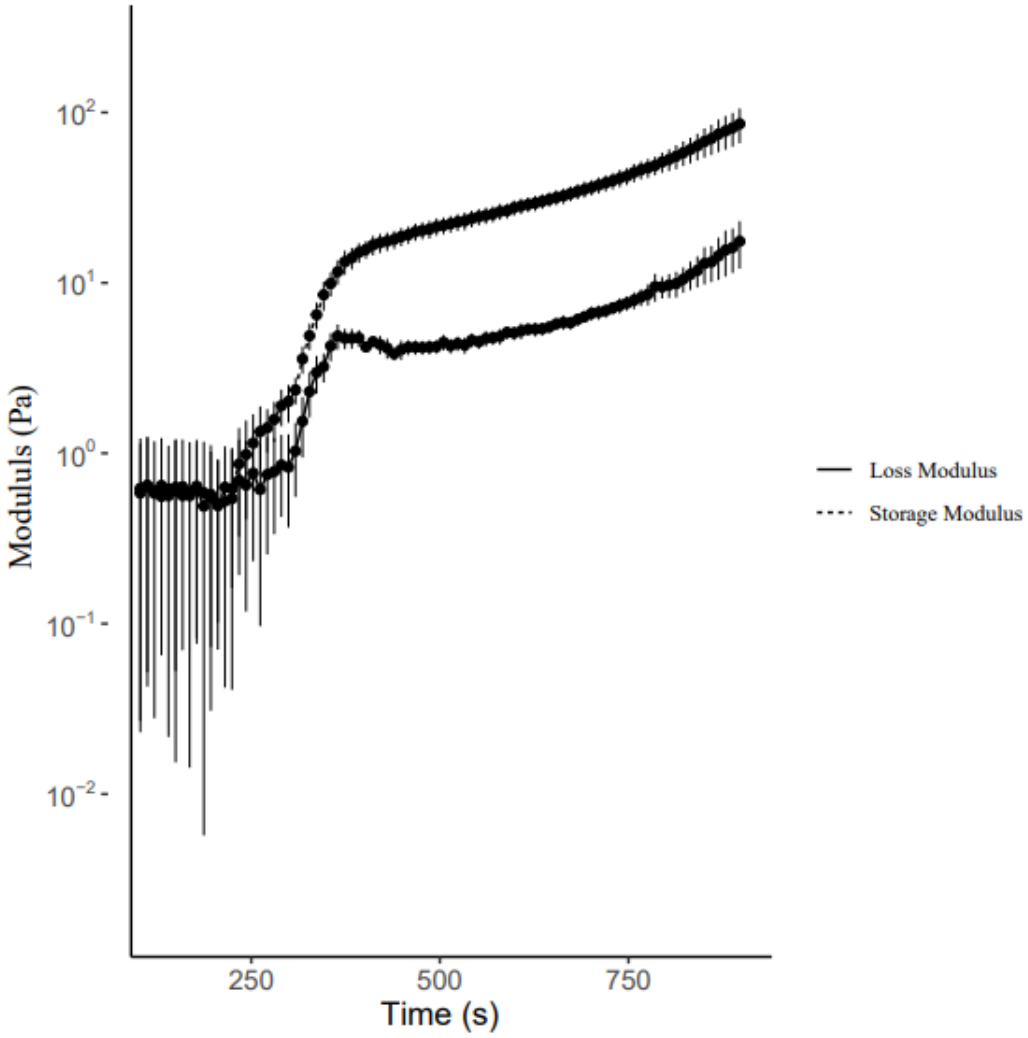

Note. Assessed by rheology with corresponding G' (Storage Modulus) and G"(Loss Modulus). Data is representative of n=3.

www.manaraa.com

Figure A6

Full panel containing hydrogels seeded with MSCs in 2D

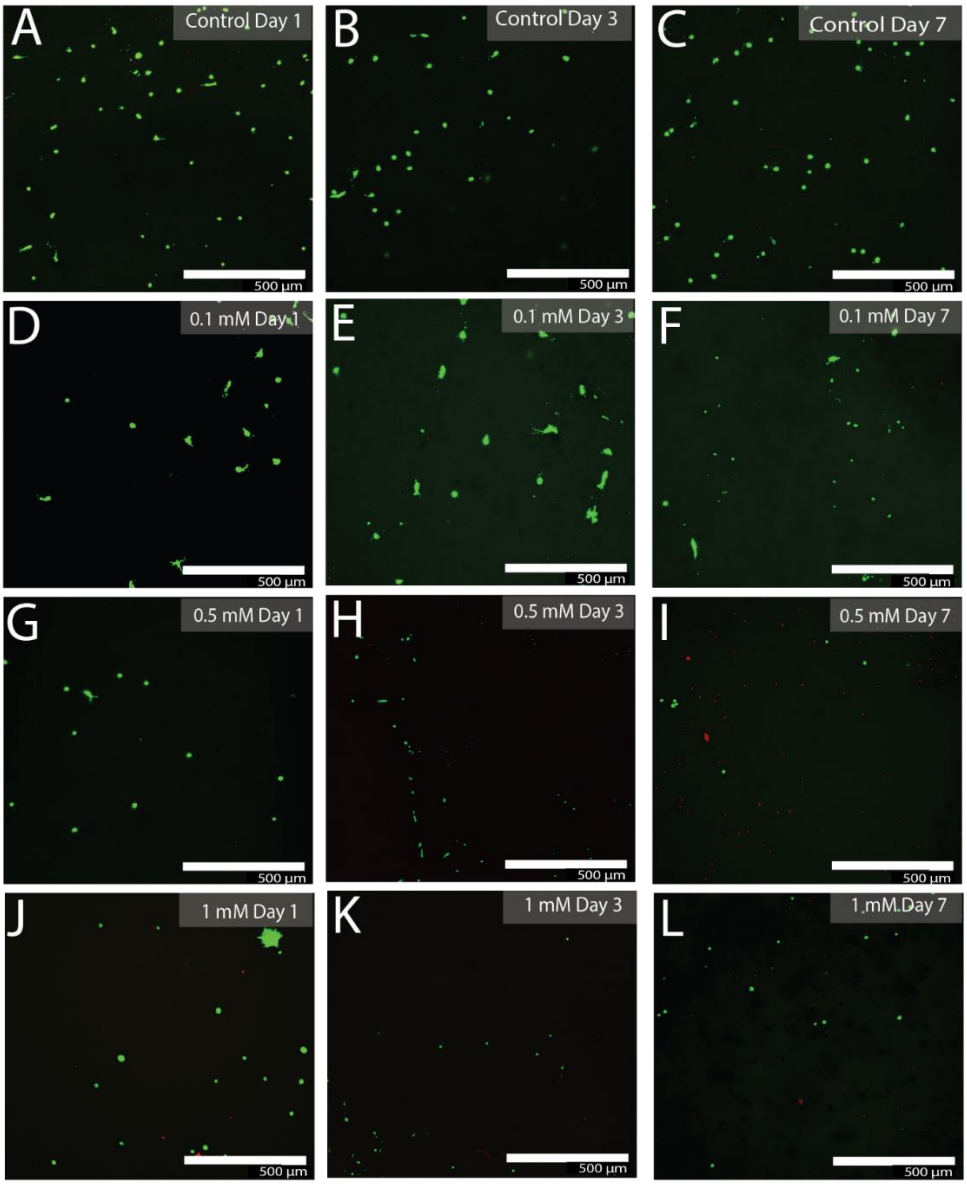

Note. Includes controls (A-C) and those crosslinked with 0.1 (D-F), 0.5 (G-I) and 1 mM genipin (J-L). The images were the results of Live/Dead assays conducted at 1, 3 and 7 days (Left, middle, and right). The images depict a Live/Dead analysis where green is representative of Calcein-AM (live cells) and red is indicative of dead cells (Edth-1). Scale bars represent 500 µm for n=1.

www.manaraa.com

Figure A7

Full panel containing hydrogels seeded with MSCs in 3D

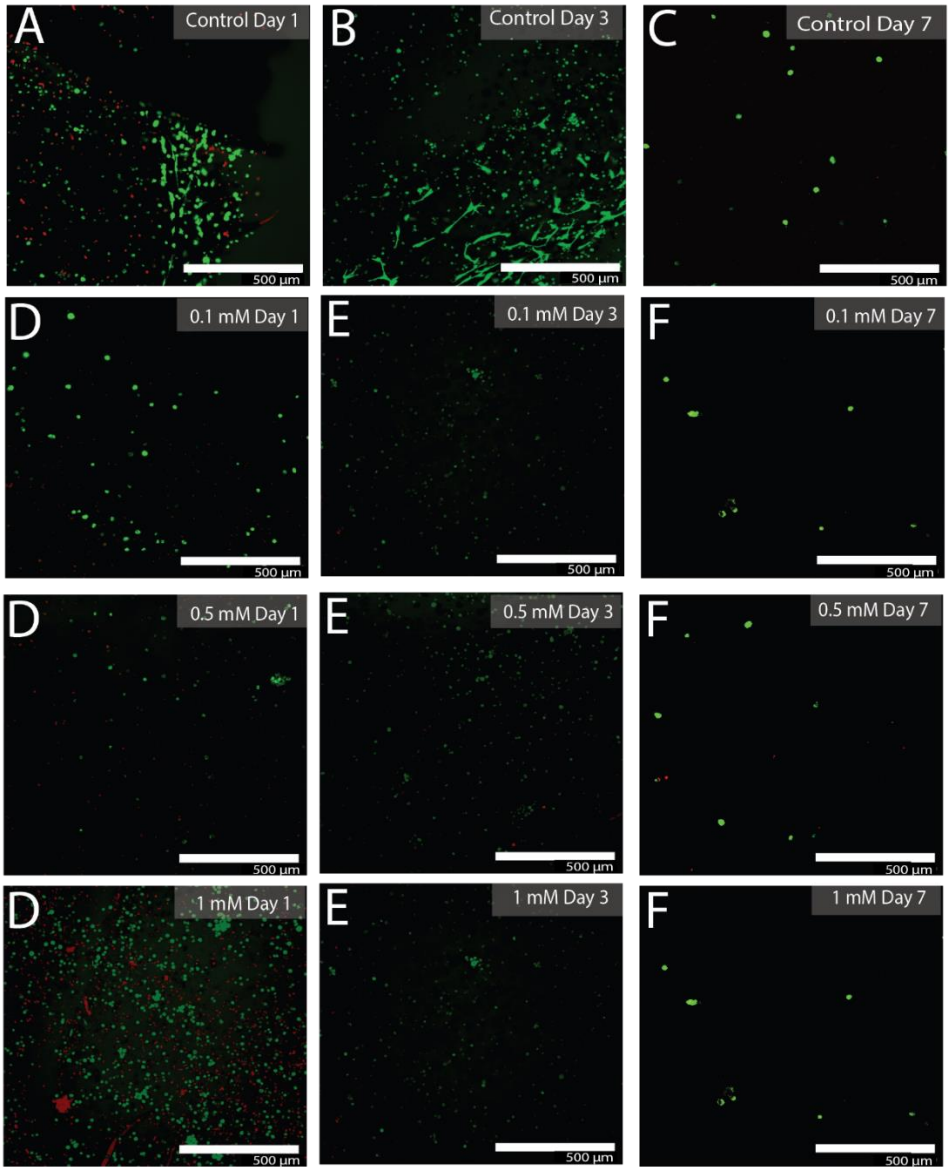

Note. Includes controls (A-C) and those crosslinked with 0.1 (D-F), 0.5 (G-I) and 1 mM genipin (J-L). The images were the results of Live/Dead assays conducted at 1, 3 and 7 days (Left, middle, and right). The images depict a Live/Dead analysis where green is representative of Calcein-AM (live cells) and red is indicative of dead cells (Edth-1). Scale bars represent 500 µm for n=5 fields of view for n=1 sample.

www.manaraa.com